AD-A041 153 NAVAL POSTGRADUATE SCHOOL MONTEREY CALIF F/G 20/4
DATA REDUCTION FOR THE UNSTEADY AERODYNAMICS ON A CIRCULATION C--ETC(U)
MAR 77 B M PICKELSIMER

UNCLASSIFIED NL

| OF |
ADA041153

END

DATE
FILMED
7-77

NAVAL POSTGRADUATE SCHOOL
Monterey, California

THESIS

DATA REDUCTION FOR THE UNSTEADY AERODYNAMICS ON A CIRCULATION CONTROL AIRFOIL

by

Billy Murel Pickelsimer

March 1977

Thesis Advisor: Louis V. Schmidt

Approved for public release; distribution unlimited.

UNCLASSIFIED

SECURITY CLASSIFICATION OF THIS PAGE (When Data Entered)

REPORT DOCUMENTATION PAGE		READ INSTRUCTIONS BEFORE COMPLETING FORM
1. REPORT NUMBER	2. GOVT ACCESSION NO.	3. RECIPIENT'S CATALOG NUMBER
4. TITLE (and Subtitle) Data Reduction for the Unsteady Aerodynamics on a Circulation Control Airfoil,		5. TYPE OF REPORT & PERIOD COVERED Master's Thesis, March 1977 6. PERFORMING ORG. REPORT NUMBER
7. AUTHOR(s) Billy Murel Pickelsimer		8. CONTRACT OR GRANT NUMBER(s)
9. PERFORMING ORGANIZATION NAME AND ADDRESS Naval Postgraduate School Monterey, California 93940		10. PROGRAM ELEMENT, PROJECT, TASK AREA & WORK UNIT NUMBERS 61 p.
11. CONTROLLING OFFICE NAME AND ADDRESS Naval Postgraduate School Monterey, California 93940		12. REPORT DATE March 1977 13. NUMBER OF PAGES 61
14. MONITORING AGENCY NAME & ADDRESS(if different from Controlling Office) Naval Postgraduate School Monterey, California 93940		15. SECURITY CLASS. (of this report) Unclassified 15a. DECLASSIFICATION/DOWNGRADING SCHEDULE

16. DISTRIBUTION STATEMENT (of this Report)

Approved for public release, distribution unlimited.

17. DISTRIBUTION STATEMENT (of the abstract entered in Block 20, if different from Report)

18. SUPPLEMENTARY NOTES

19. KEY WORDS (Continue on reverse side if necessary and identify by block number)

20. ABSTRACT (Continue on reverse side if necessary and identify by block number)

Calculating the lift, drag, and pitching moment coefficients for an airfoil from the static pressure distribution obtained from wind tunnel tests is routine task when steady flow is considered, but it is much more complicated when the airfoil is operating in an unsteady flow field, similar to that experienced by a helicopter rotor blade, produced by an oscillating wind tunnel. A data reduction routine capable of condensing the large

DD FORM 1 JAN 73 1473 (Page 1)

EDITION OF 1 NOV 65 IS OBSOLETE
S/N 0102-014-6601

UNCLASSIFIED

SECURITY CLASSIFICATION OF THIS PAGE (When Data Entered)

numbers of data associated with the unsteady investigation, as well as a numerical integration algorithm for the unsteady aerodynamic coefficients, were developed; however, no unsteady data were collected due to hardware failures. The ability of the program was demonstrated on previously obtained steady and quasi-steady data and sample results were presented.

Approved for public release, distribution unlimited

Data Reduction for the Unsteady Aerodynamics on a Circulation Control Airfoil

by

Billy Murel Pickelsimer
Lieutenant, United States Navy
B.S., Oklahoma State University, 1970

Submitted in partial fulfillment of the requirements for the degree of

MASTER OF SCIENCE IN AERONAUTICAL ENGINEERING

from the

NAVAL POSTGRADUATE SCHOOL
March 1977

Author 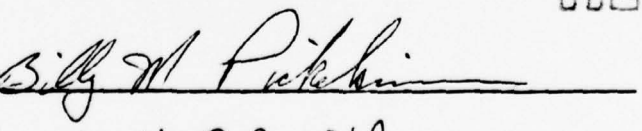

Approved by: 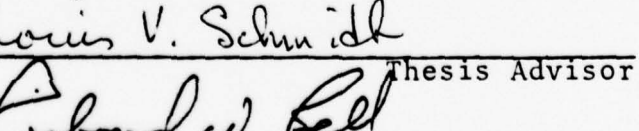
Thesis Advisor

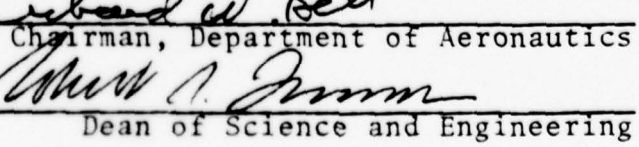
Chairman, Department of Aeronautics

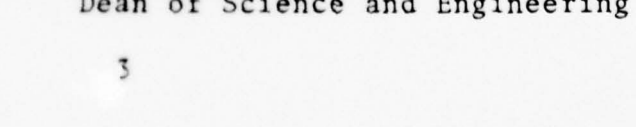
Dean of Science and Engineering

NAVAL POSTGRADUATE SCHOOL
Monterey, California

Rear Admiral Isham Linder
Superintendent

Jack R. Borsting
Provost

This thesis prepared in conjunction with research supported by the Naval Air Systems Command 370C.

Released as a
Technical Report by:

R. R. Fossum
Dean of Research

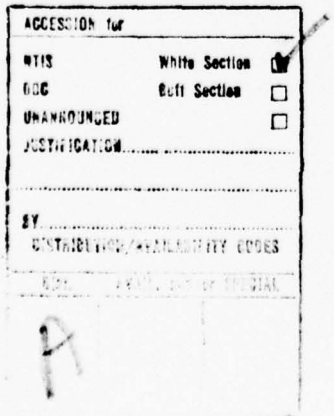

ABSTRACT

Calculating the lift, drag, and pitching moment coefficients for an airfoil from the static pressure distribution obtained from wind tunnel tests is routine task when steady flow is considered, but it is much more complicated when the airfoil is operating in an unsteady flow field, similar to that experienced by a helicopter rotor blade, produced by an oscillating wind tunnel. A data reduction routine capable of condensing the large numbers of data associated with the unsteady investigation, as well as a numerical integration algorithm for the unsteady aerodynamic coefficients, were developed; however, no unsteady data were collected due to hardware failures. The ability of the program was demonstrated on previously obtained steady and quasi-steady data and sample results were presented.

TABLE OF CONTENTS

LIST OF TABLES

LIST OF FIGURES

LIST OF SYMBOLS

C	Chord Length
C_c	Coefficient of Chord Force
C_d	Coefficient of Drag
C_l	Coefficient of Lift
C_m	Coefficient of Pitching Moment
C_n	Coefficient of Normal Force
C_p	Coefficient of Pressure
C_μ	Coefficient of Momentum Blowing
$\|Gf\|$	Transfer Function Gain
Hz	Hertz
ϕ	Phase Angle (Phi)
RMS	Root Mean Square
U	Velocity
W	Frequency
X	Horizontal Reference Coordinate
Y	Vertical Reference Coordinate
$\langle\ ^2\rangle^{\frac{1}{2}}$	RMS

I. INTRODUCTION

The primary objectives of this investigation were: 1) to report on the data reduction techniques used to obtain values for both steady and non-steady aerodynamic coefficients, resulting from the experimentally acquired static pressure distribution over the model when the tunnel was operating at a specified dynamic pressure, with Coanda blowing oscillated at various frequencies and amplitudes of momentum blowing coefficient; and 2) to present a sample of results. Removal of the model from the tunnel for modifications in November 1976 precluded any actual processing of non-steady data consistent with the stated goals.[1]

However, the data reduction techniques are applicable to the pressure distribution obtained with steady Coanda blowing and will be demonstrated on such data obtained in April 1976. Prior to removal of the model, the tunnel was operated without blowing in an effort to generate a set of non-steady data to be used in tailoring the data reduction procedures to be used downstream in the on-going project. In that test, the model experienced self-excited harmonic pressures resulting from vortices being shed alternately

---

[1]The modifications, to correct for surface delaminations near the upper jet nozzle, include a steel upper surface trailing edge and slot height adjustment to 0.015 inches. Additional pressure taps were installed on the upper surface forward of the Coanda slot, and leaking tubes were repaired while the modifications were being implemented.

from the upper and lower surfaces. The manually recorded data consisted of the RMS and mean values of the unsteady pressure, and the phase angle in respect to a reference for each pressure orifice. A more complete description of the data acquisition system is given in Section II B.

II. EQUIPMENT AND INSTRUMENTATION

A. AIRFOIL

The airfoil used in this study was obtained from the Lockheed-California Company after completion of their design feasibility study on circulation control rotors (Ref.1). It had an elliptical cross-section with a chord of 10.215 inches, thickness ratio of 0.20, and camber of 3.3% (Figure 1). A slot to facilitate Coanda blowing was machined in the upper surface at chord position X/C=0.95, with the slot height set at 0.010 inches. Coanda air was supplied to the plenum cavity at both ends of the section to insure uniform flow along the span. Fifty-three pressure taps at mid-span with a chord-wise orientation were monitored through two scanivalve transducers for an electrical representation of the pressure distribution over the airfoil. The pressure tap locations are listed in Table I.

The 2.0 x 2.0 foot unsteady flow wind tunnel in the Department of Aeronautics Laboratories at the Naval Postgraduate School was used as it is capable of simulating the velocity flow field experienced by blade elements of a helicopter in forward flight. The model was mounted at an angle of attack of -5 degrees, which closely corresponds to the zero-lift angle of attack for the data reported herein.

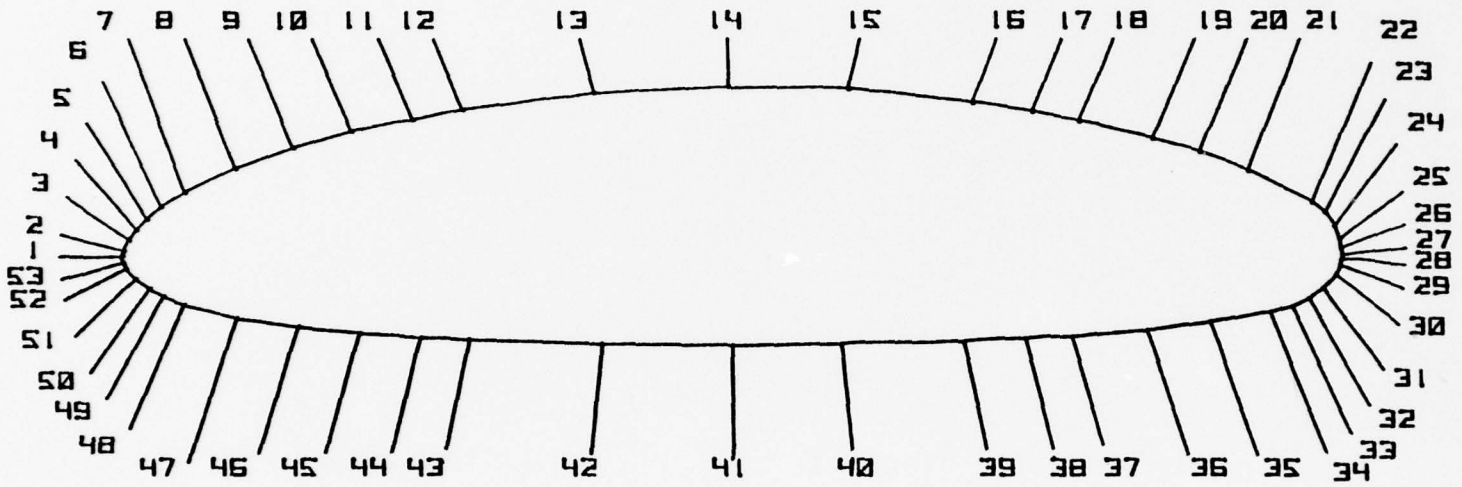

FIGURE 1
AIRFOIL CROSS-SECTION WITH TAP LOCATIONS

TABLE I

AIRFOIL PRESSURE TAP LOCATIONS

TAP #	X	Y	TAP #	X	Y
1	0.000	0.000	28	10.206	-0.020
2	0.009	0.050	29	10.162	-0.040
3	0.055	0.135	30	10.118	-0.152
4	0.123	0.220	31	10.051	-0.255
5	0.211	0.305	32	9.940	-0.372
6	0.327	0.400	33	9.800	-0.400
7	0.525	0.518	34	9.613	-0.443
8	0.954	0.710	35	9.114	-0.525
9	1.441	0.875	36	8.587	-0.590
10	1.931	1.004	37	7.960	-0.638
11	2.435	1.066	38	7.570	-0.658
12	2.851	1.182	39	7.059	-0.678
13	3.958	1.315	40	6.033	-0.700
14	5.086	1.360	41	5.116	-0.708
15	6.096	1.343	42	4.019	-0.695
16	7.132	1.238	43	2.902	-0.665
17	7.627	1.162	44	2.496	-0.645
18	8.019	1.088	45	1.992	-0.610
19	8.635	0.950	46	1.478	-0.560
20	9.028	0.844	47	0.964	-0.490
21	9.430	0.552	48	0.521	-0.388
22	9.964	0.440	49	0.349	-0.320
23	10.070	0.340	50	0.230	-0.260
24	10.140	0.220	51	0.115	-0.178
25	10.191	0.147	52	0.034	-0.098
26	10.199	0.073	53	0.010	-0.052
27	10.215	0.000			

X IN INCHES AFT OF LEADING EDGE

Y IN INCHES FROM CHORD LINE

B. INSTRUMENTATION

The data acquisition system evolved from a classic manometer board arrangement with readings hand recorded (Ref. 2) and reduced to the present system, which employed electrical read-outs with an existing Digitec system with customized signal conditioning. The digital multiplexing circuitry in the Digitec system was interconnected through the scanivalve solenoid controllers for automatic scanivalve advancing as the output of the digital voltmeter was sequentially printed on a paper tape. Pressure sensing was accomplished by connecting each of the pressure taps to one of the two scanivalves (Figure 2) through tubing of uniform diameter and length. This was done to insure a constant transfer function for all pressure taps, when measuring unsteady pressures. Calibration tests using the method reported by Johnson (Ref.3) showed an acceptable variation in dynamic gain in the frequency range from 0 to 300 Hz (Figure 3), which included the range of practical interest.

For the unsteady aerodynamics analysis (C_μ=0), the voltage representation of the surface static pressures was of the form

$$e_x = a_x + b_x(t). \qquad (2.1)$$

Full analog measuring techniques were employed in measuring the mean voltage, RMS voltage, and phase relationship to a reference for each pressure tap. The mean voltage was obtained by processing the signal through a low-pass filter circuit (Figure 4) with a two second time constant which

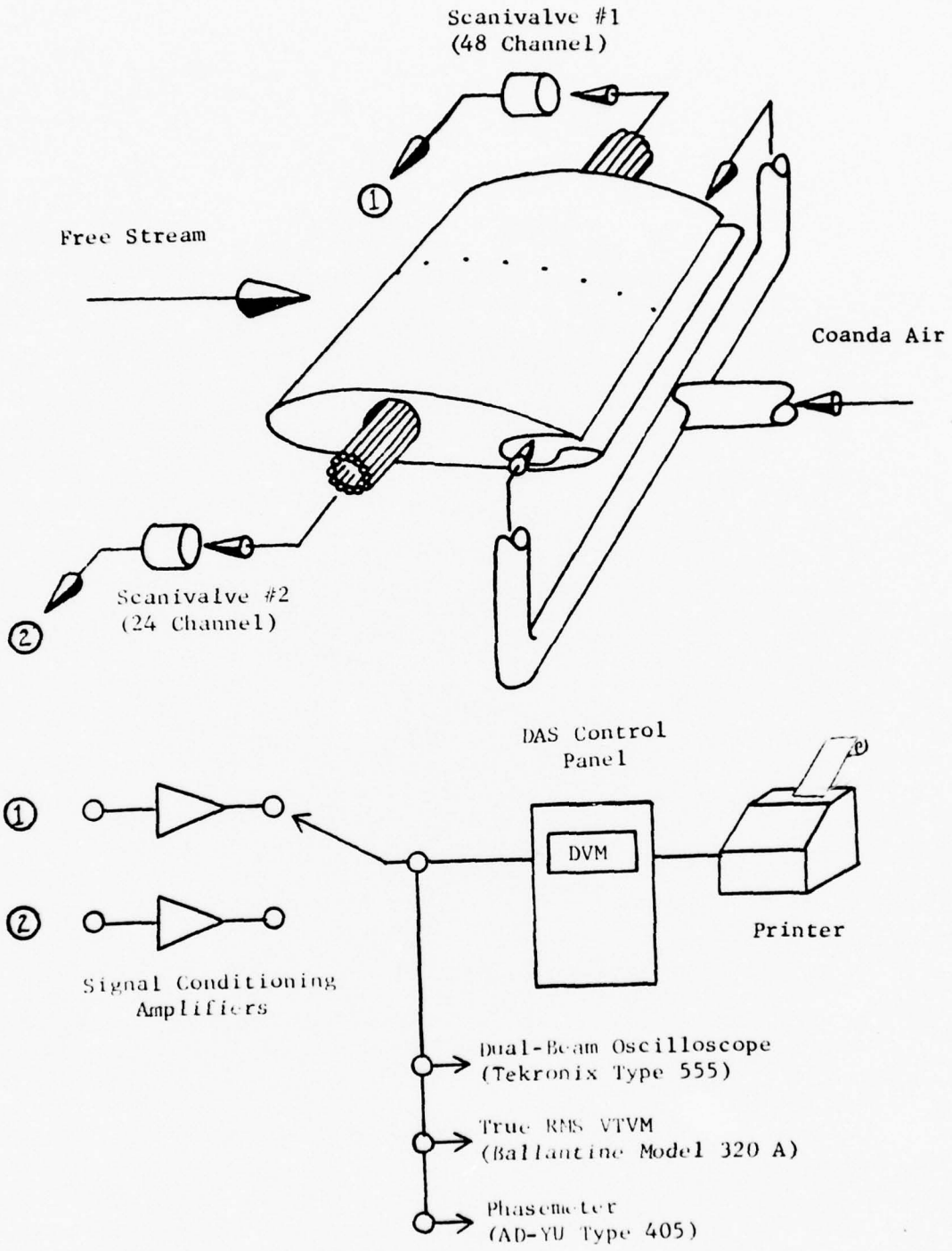

Figure 2
Airfoil Instrumentation

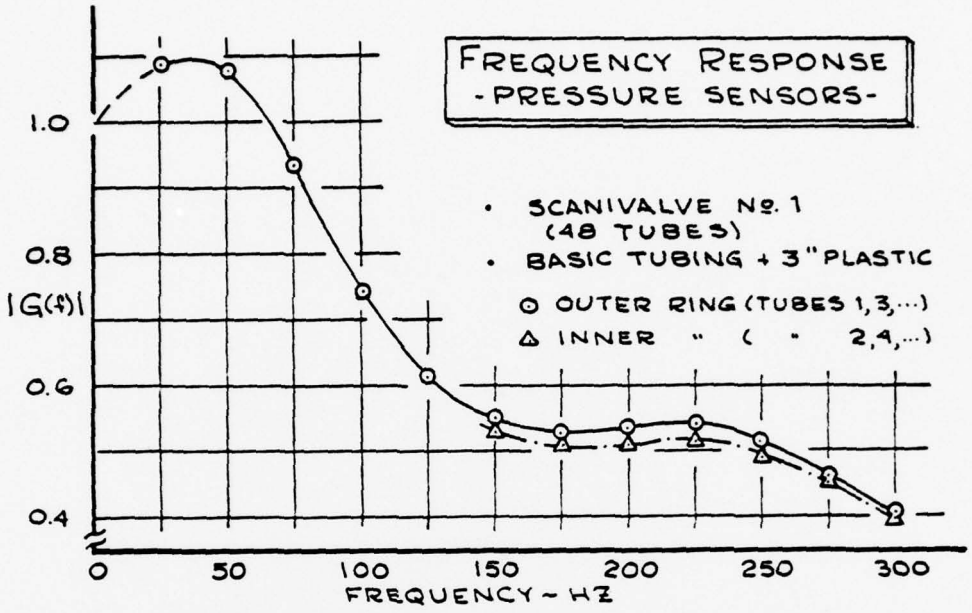
FREQUENCY RESPONSE
-PRESSURE SENSORS-
• SCANIVALVE Nº. 1
(48 TUBES)
• BASIC TUBING + 3" PLASTIC
⊙ OUTER RING (TUBES 1, 3, ···)
△ INNER " (" 2, 4, ···)
1.0
0.8
|G(f)|
0.6
0.4
0
50
100
150
200
250
300
FREQUENCY ~ HZ

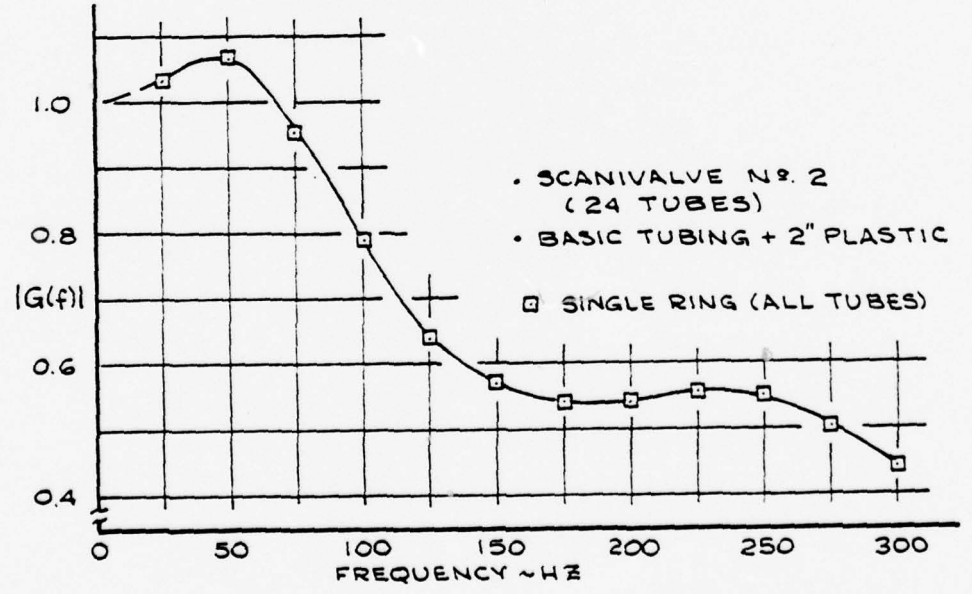
• SCANIVALVE Nº. 2
(24 TUBES)
• BASIC TUBING + 2" PLASTIC
□ SINGLE RING (ALL TUBES)
1.0
0.8
|G(f)|
0.6
0.4
0
50
100
150
200
250
300
FREQUENCY ~ HZ

Figure 3

corresponds to a corner frequency of 0.08 Hz on a Bode plot. Therefore, the influence of the unsteady voltage was essentially negated and the output readings represented the steady components of the signal.

C. ADVANCED DATA ACQUISITION SYSTEM

To meet the primary objective mentioned in Section I, a more sophisticated data acquisition and reduction system will be required and is now being constructed by Englehardt[2] at the Naval Postgraduate School in the Department of Aeronautics. The system, based on the Intel MDS-80 microprocessor unit, will control the logic of the experiment, collect and store data, and handle the entire data reduction process. The algorithm for data reduction discussed in Section V was proven sufficiently simple and capable of performing all required data reduction and numerical integration.

---

[2]Master of Science thesis by Englehardt with a complete description of the entire microprocessor system will be published in June 1977.

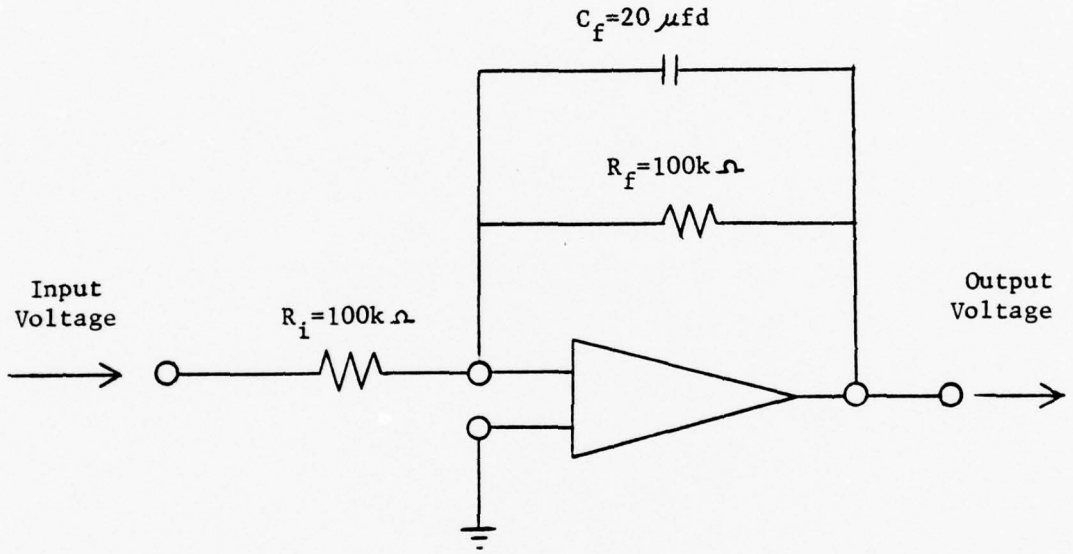

Figure 4
Low-Pass Filter Circuit

III. DATA REDUCTION

A. STEADY DATA PROCESSING

The aerodynamic coefficients are defined by integral equations but must be approximated by numerical integrations, since data are available only at a finite number of pressure tap locations. The approximate steady normal force, chord force, and pitching moment coefficients are

$$C_n = \int_0^{1.0} (C_{p_l} - C_{p_u}) d(X/C)$$

$$C_c = \int_{Y/C\ (min)}^{Y/C\ (max)} (C_{p_f} - C_{p_r}) d(Y/C) \qquad (3.1)$$

$$C_{m(TE)} = \int_{-Y/C\ (min)}^{Y/C\ (max)} (C_{p_f} - C_{p_r})(Y/C) d(Y/C) + \int_0^{1.0} (C_{p_l} - C_{p_u})(1 - X/C) d(X/C)$$

Then, with an angle of attack correction for the force coefficients and a moment transfer to the quarter-chord position, the aerodynamic coefficients are

$$C_l = C_n \cos\alpha - C_c \sin\alpha$$

$$C_d = C_n \sin\alpha + C_c \cos\alpha \qquad (3.2)$$

$$C_{m(c/4)} = C_{m(TE)} - 0.75 C_n .$$

The pressure data from the April 1976 tests and the November 1976 mean pressure data were transferred to a

Hewlett-Packard 9830 tape cassette and processed using the program listed in Appendix A, which employs the equivalent numerical relationship to the equations stated above.

B. UNSTEADY DATA PROCESSING

Before the unsteady data were suitable for numerical integration, a dynamic gain correction was necessary to account for the transfer function discussed in Section II. The frequency of the self-induced oscillations was constant at 262 Hz when the tunnel airspeed was approximately 100 ft/s. From Figure 3, the corresponding gain correction, $|G_f|$, was approximately 0.5, which implied that the amplitude of the surface static pressure was attenuated by a factor of one-half at the transducer. All phase angle values were relative to tube number 7, which was arbitrarily chosen as a clock reference. Phase angle errors resulting from the two different scanivalve circuits were faired out in the analysis (Figure 5).

With the above corrections, the numerical integration of the unsteady static pressure distribution was carried out in a manner similar to the steady pressure integrations. For the unsteady normal force coefficient

$$\langle C_n^2 \rangle^{\frac{1}{2}} \sin\phi = \int_0^{1.0} (C_{p_l} \sin\phi - C_{p_u} \sin\phi) d(X/C)$$

$$\langle C_n^2 \rangle^{\frac{1}{2}} \cos\phi = \int_0^{1.0} (C_{p_l} \cos\phi - C_{p_u} \cos\phi) d(X/C) \qquad (3.3)$$

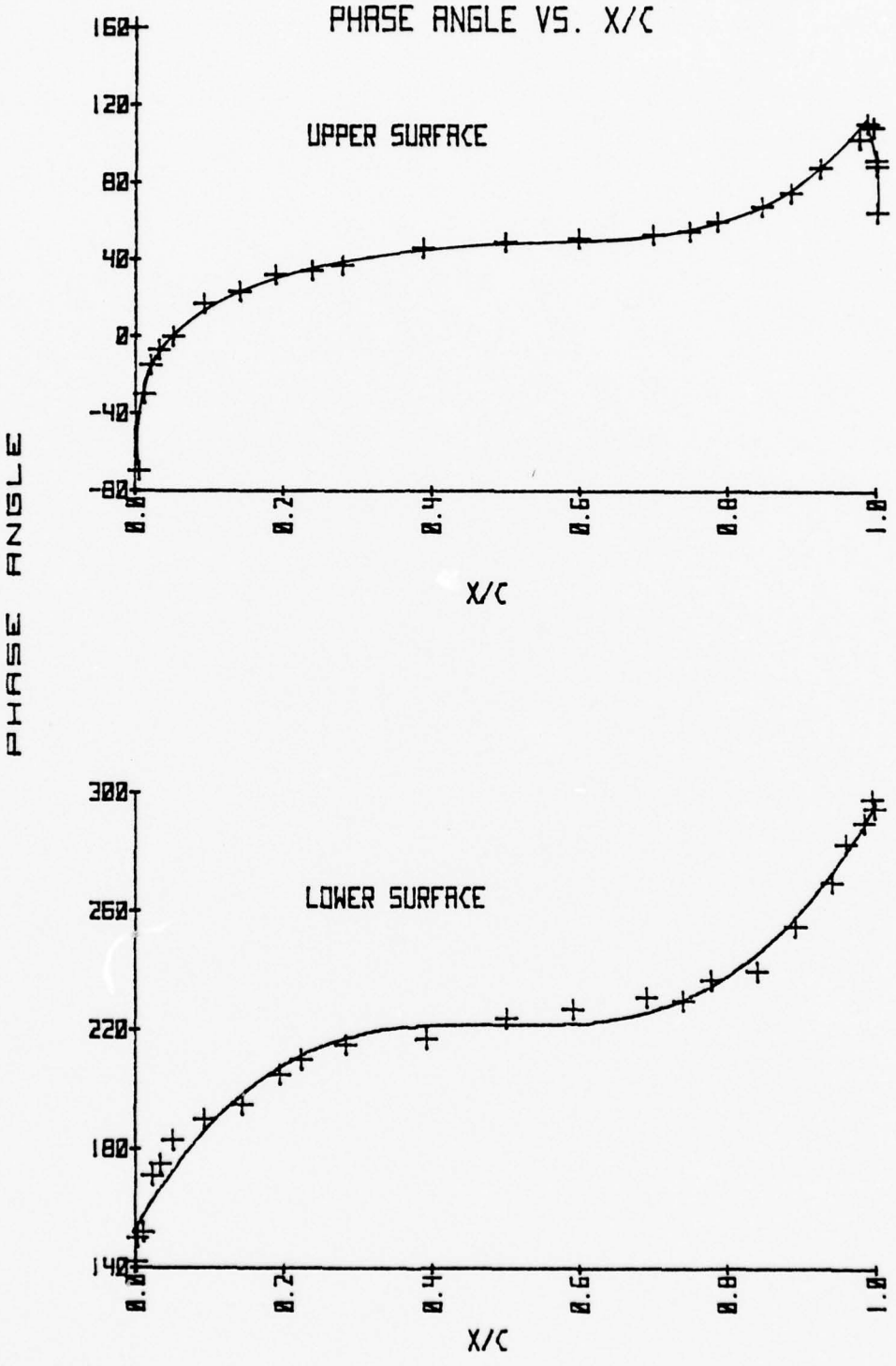
PHASE ANGLE VS. X/C
UPPER SURFACE
160
120
80
40
0
-40
-80
0.0
0.2
0.4
0.6
0.8
1.0
X/C
PHASE ANGLE
LOWER SURFACE
300
260
220
180
140
0.0
0.2
0.4
0.6
0.8
1.0
X/C

Figure 5

Then $$\langle C_n^2 \rangle^{\frac{1}{2}} = \sqrt{(\langle C_n^2 \rangle^{\frac{1}{2}} \sin\phi)^2 + (\langle C_n^2 \rangle^{\frac{1}{2}} \cos\phi)^2}$$

And $$\phi_T = \tan^{-1} \frac{(\langle C_n^2 \rangle^{\frac{1}{2}} \sin\phi)}{(\langle C_n^2 \rangle^{\frac{1}{2}} \cos\phi)}$$

where $\langle C_n^2 \rangle^{\frac{1}{2}}$ is the RMS value of the normal force coefficient and ϕ_T is the phase angle relative to tube number 7. The chord force and pitching moment coefficients were calculated similarly.

$$\langle C_c^2 \rangle^{\frac{1}{2}} \sin\phi = \int_{-Y/C(\min)}^{Y/C(\max)} (C_{p_f} \sin\phi - C_{p_r} \sin\phi) d(Y/C)$$

$$\langle C_c^2 \rangle^{\frac{1}{2}} \cos\phi = \int_{-Y/C(\min)}^{Y/C(\max)} (C_{p_f} \cos\phi - C_{p_r} \cos\phi) d(Y/C)$$

$$\langle C_c^2 \rangle^{\frac{1}{2}} = \sqrt{(\langle C_c^2 \rangle^{\frac{1}{2}} \sin\phi)^2 + (\langle C_c^2 \rangle^{\frac{1}{2}} \cos\phi)^2}, \quad \phi_T = \frac{(\langle C_c^2 \rangle^{\frac{1}{2}} \sin\phi)}{(\langle C_c^2 \rangle^{\frac{1}{2}} \cos\phi)}$$

$$\langle C_m^2 \rangle_{te}^{\frac{1}{2}} \sin\phi = \int_{-Y/C(\min)}^{Y/C(\max)} (C_{p_f} \sin\phi - C_{p_r} \sin\phi)(Y/C) d(Y/C) +$$

$$\int_0^{1.0} (C_{p_l} \sin\phi - C_{p_u} \sin\phi)(1 - X/C) d(X/C)$$

$$\langle C_m^2 \rangle_{te}^{\frac{1}{2}} \cos\phi = \int_{-Y/C(min)}^{Y/C(max)} (C_{p_f} \cos\phi - C_{p_r} \cos\phi)(Y/C) d(Y/C) \quad +$$

$$\int_0^1 (C_{p_l} \cos\phi - C_{p_u} \cos\phi)(1 - X/C) d(X/C)$$

$$\langle C_m^2 \rangle_{te}^{\frac{1}{2}} = \sqrt{(\langle C_m^2 \rangle^{\frac{1}{2}} \sin\phi)^2 + (\langle C_m^2 \rangle^{\frac{1}{2}} \cos\phi)^2} \quad , \quad \phi_T = \frac{(\langle C_m^2 \rangle^{\frac{1}{2}} \sin\phi)}{(\langle C_m^2 \rangle^{\frac{1}{2}} \cos\phi)}$$

The unsteady aerodynamic coefficients are calculated as in Eqs. 3.2, with the aid of elementary trigonometric identities to account for the phase angles. The program listed in Appendix A has the option for unsteady numerical integration incorporated.

It is intended that the $C_\mu = 0$ oscillating pressure measurements be repeated when the improved data acquisition system becomes available. The tests will be conducted at several tunnel dynamic pressures to determine the Reynolds number dependence of the data. The previous measurements were at approximately $R_e = 0.54 \times 10^6$.

IV. RESULTS

A. STEADY DATA RESULTS

The validity of the concept of circulation control was demonstrated by Englar (Refs. 4 and 5) and is confirmed here with the steady momentum blowing coefficient results. The resulting aerodynamic coefficients are summarized in Table II. The ability to produce relatively large increases in lift coefficient with only a small increase in blowing coefficient, shown graphically in Figures 6a, b, and c, is one of the desirable characteristics of the system. Probably the best measure of the effectiveness is the aerodynamic lift amplification ratio, $\partial C_l/\partial C_\mu$, which was computed to be approximately 15.3, the low value being attributed to the geometric deficiencies of the trailing edge slot as alluded to in Section I. However, the results are encouraging.

Close scrutiny of the coefficient of pressure information plotted against X/C (Figures 7-12) reveals a pressure distribution over the model such that the center of pressure was at the mid-chord position, which is in agreement with the theory. The center of pressure position is also verified by the graph of $C_{m(c/4)}$ Vs. C_μ.

$$\left(\frac{X}{C}\right)_{C.P.} = \frac{C}{4} - \frac{(\partial C_m/\partial C_\mu)}{(\partial C_l/\partial C_\mu)} = .25 - \frac{(-3.5)}{(15.3)} = .48$$

TABLE II

AERODYNAMIC COEFFICIENT SUMMARY

STEADY AERODYNAMIC COEFFICIENTS

Angle of Attack=-5 degrees U=100 ft/s

Run No.	C_μ	C_l	C_d	$C_{m(c/4)}$
42301	0	-0.0942	0.0341	-0.1065
42302	0.0855	1.0332	0.1083	-0.3907
42303	0.0640	0.8146	0.0678	-0.3365
42304	0.0448	0.5774	0.0440	-0.2776
42305	0.0272	0.3459	0.0327	-0.2175
43206	0.0133	0.1100	0.0367	-0.1664

UNSTEADY AERODYNAMIC COEFFICIENTS

C_l=-0.0765	C_l(RMS)=2.1404	ϕ=225 degrees
C_d= 0.0451	C_d(RMS)=0.1629	ϕ= 39 degrees
C_m=-0.1063	C_m(RMS)=0.5817	ϕ= 63 degrees

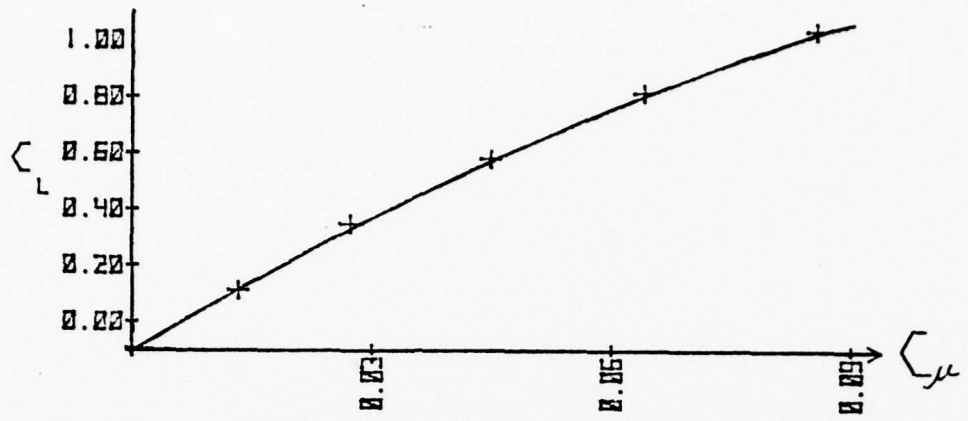

FIGURE 6A

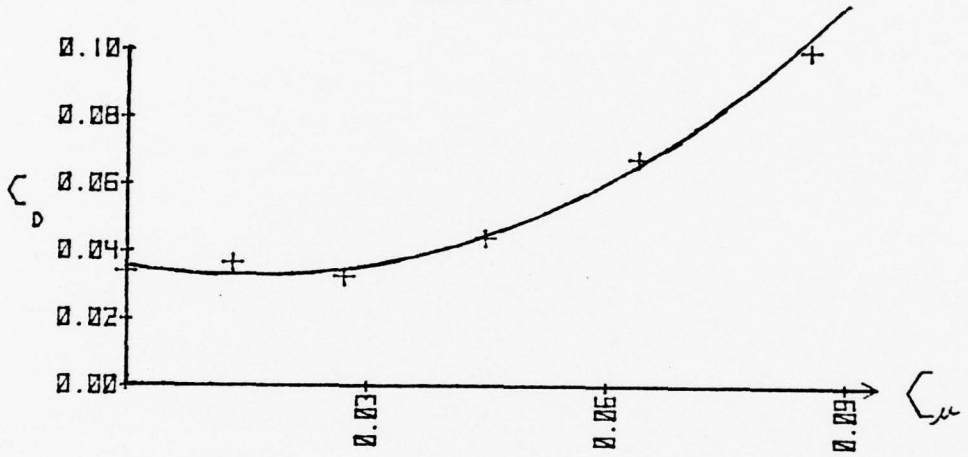

FIGURE 6B

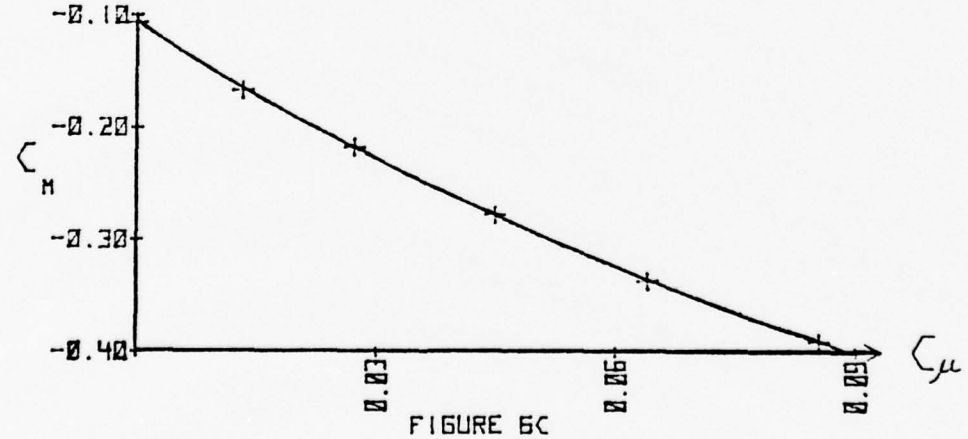

FIGURE 6C

STEADY AERODYNAMIC COEFFICIENT VARIATION WITH C_μ

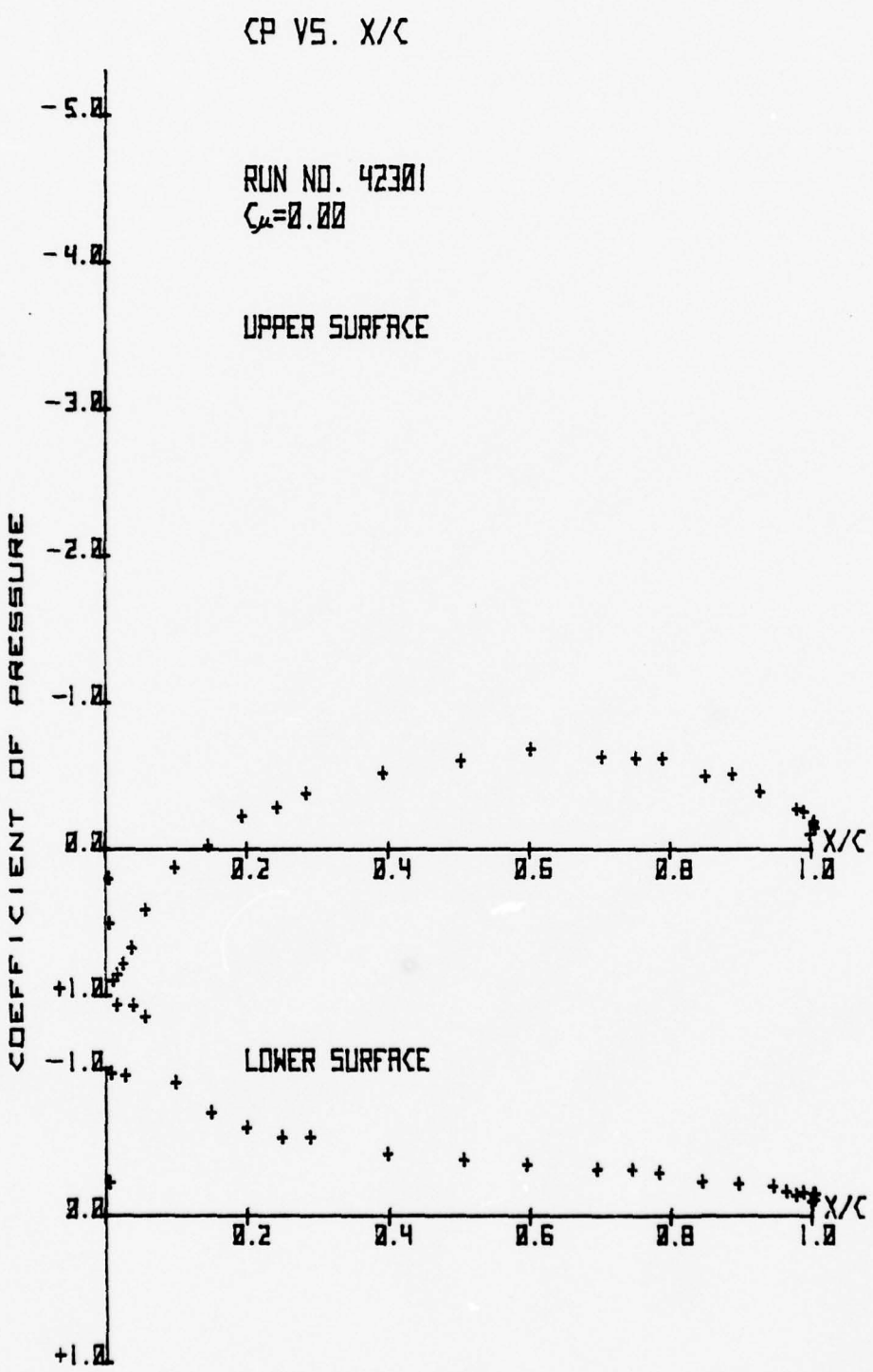
CP VS. X/C
RUN NO. 42301
Cμ=0.00
UPPER SURFACE
LOWER SURFACE
COEFFICIENT OF PRESSURE
-5.0
-4.0
-3.0
-2.0
-1.0
0.0
+1.0
-1.0
0.0
+1.0
0.2
0.4
0.6
0.8
1.0
X/C
X/C

Figure 7

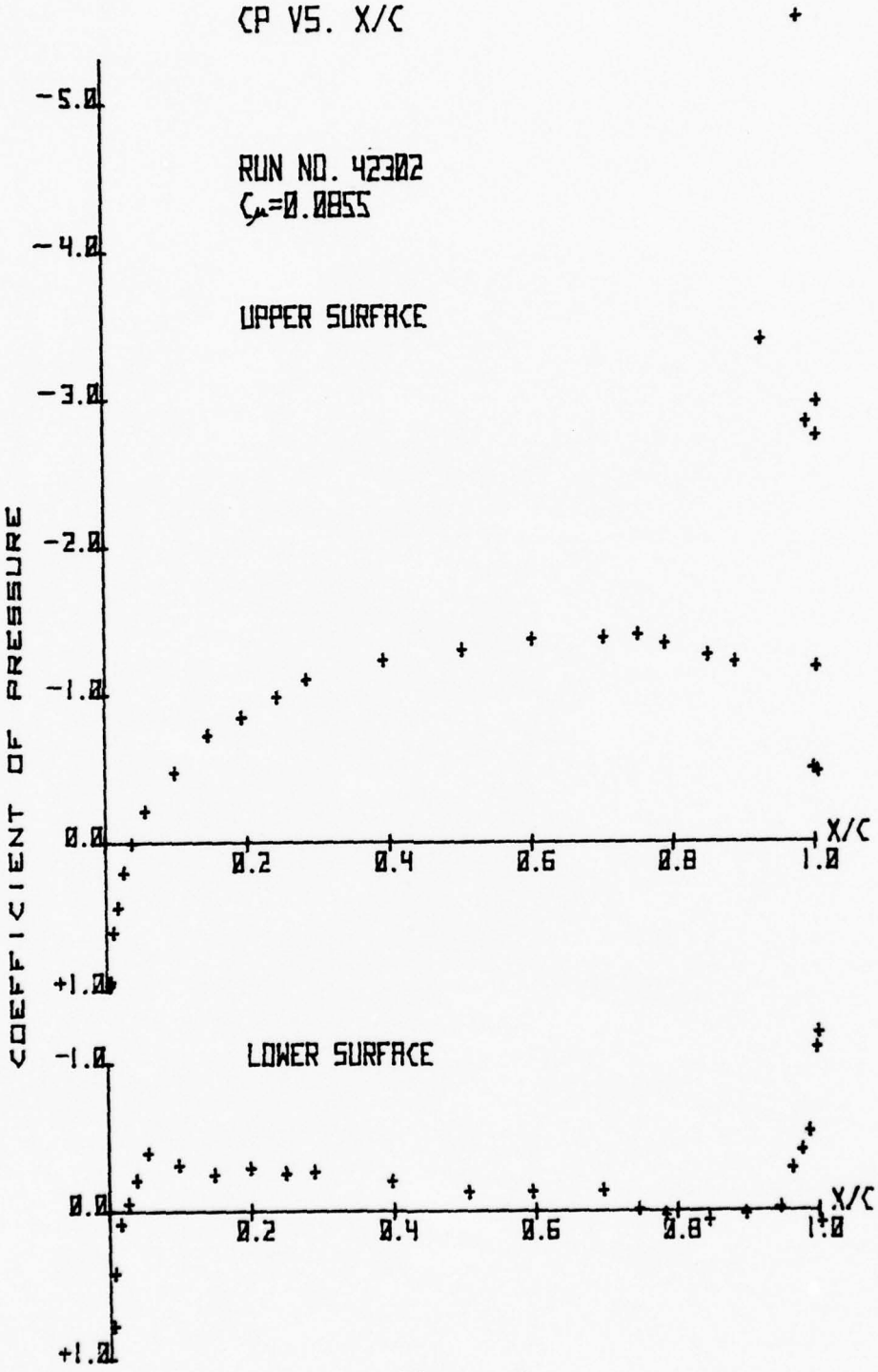
CP VS. X/C
RUN NO. 42302
C_μ=0.0855
UPPER SURFACE
LOWER SURFACE
COEFFICIENT OF PRESSURE
-5.0
-4.0
-3.0
-2.0
-1.0
0.0
+1.0
-1.0
0.0
+1.0
0.2
0.4
0.6
0.8
1.0
X/C
X/C

Figure 8

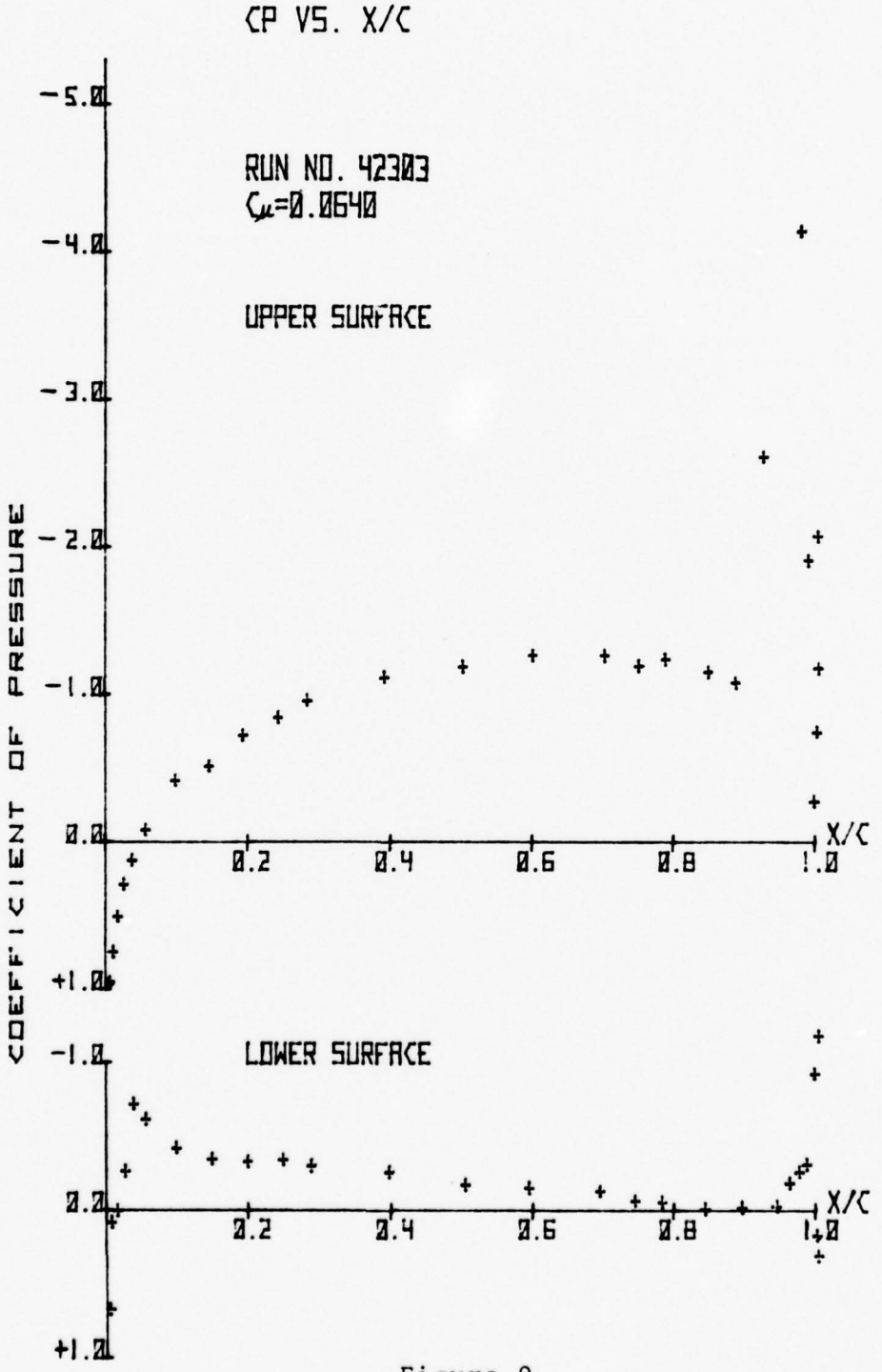
CP VS. X/C
RUN NO. 42303
Cμ=0.0640
UPPER SURFACE
LOWER SURFACE
COEFFICIENT OF PRESSURE
-5.0
-4.0
-3.0
-2.0
-1.0
0.0
+1.0
-1.0
0.0
+1.0
0.2
0.4
0.6
0.8
1.0
X/C
X/C

Figure 9

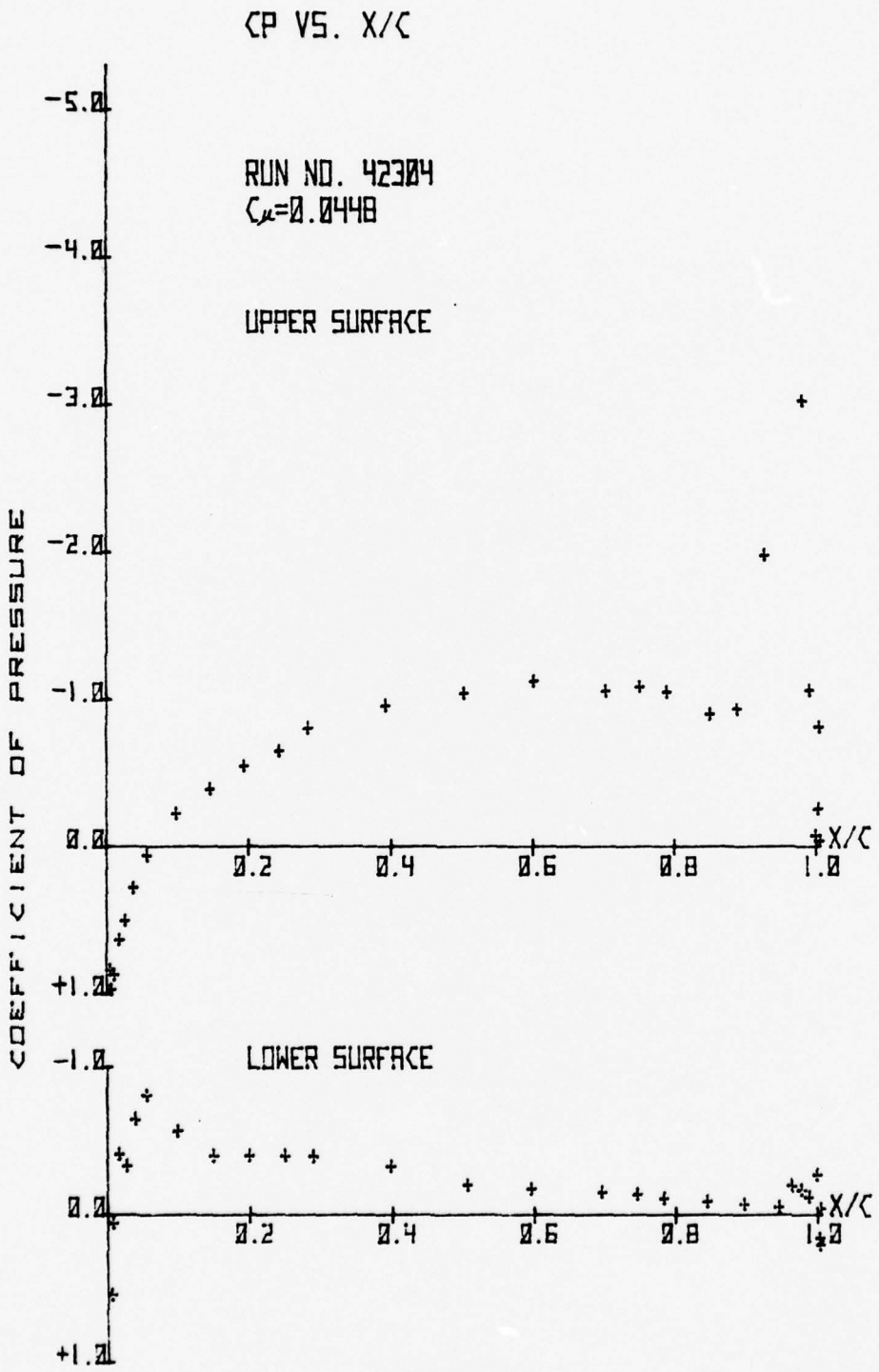
CP VS. X/C
RUN NO. 42304
Cμ=0.0448
UPPER SURFACE
LOWER SURFACE
COEFFICIENT OF PRESSURE
-5.0
-4.0
-3.0
-2.0
-1.0
0.0
+1.0
0.2
0.4
0.6
0.8
1.0
X/C

Figure 10

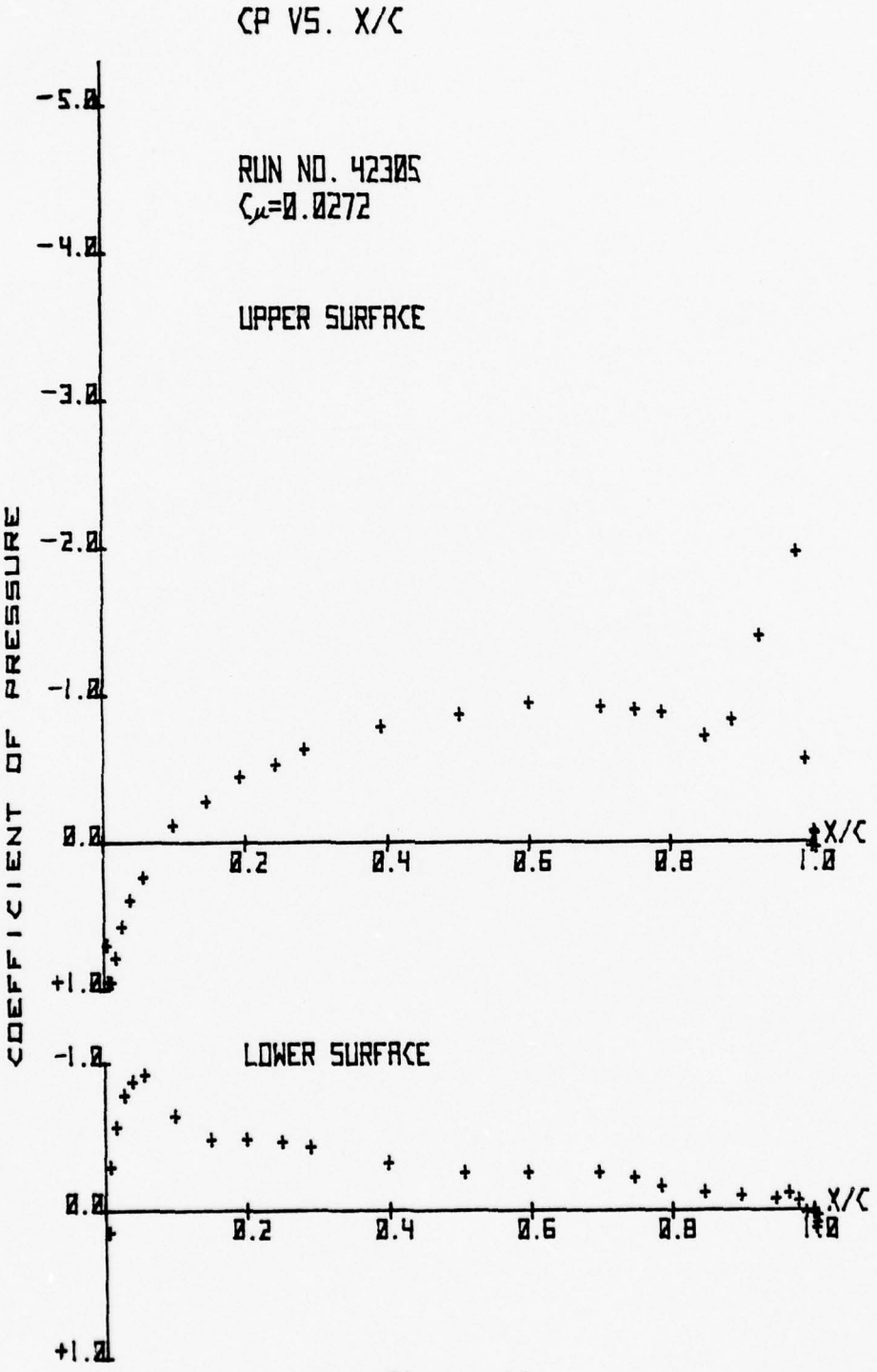
CP VS. X/C
RUN NO. 42305
Cμ=0.0272
UPPER SURFACE
LOWER SURFACE
COEFFICIENT OF PRESSURE
-5.0
-4.0
-3.0
-2.0
-1.0
0.0
+1.0
0.2
0.4
0.6
0.8
1.0
X/C

Figure 11

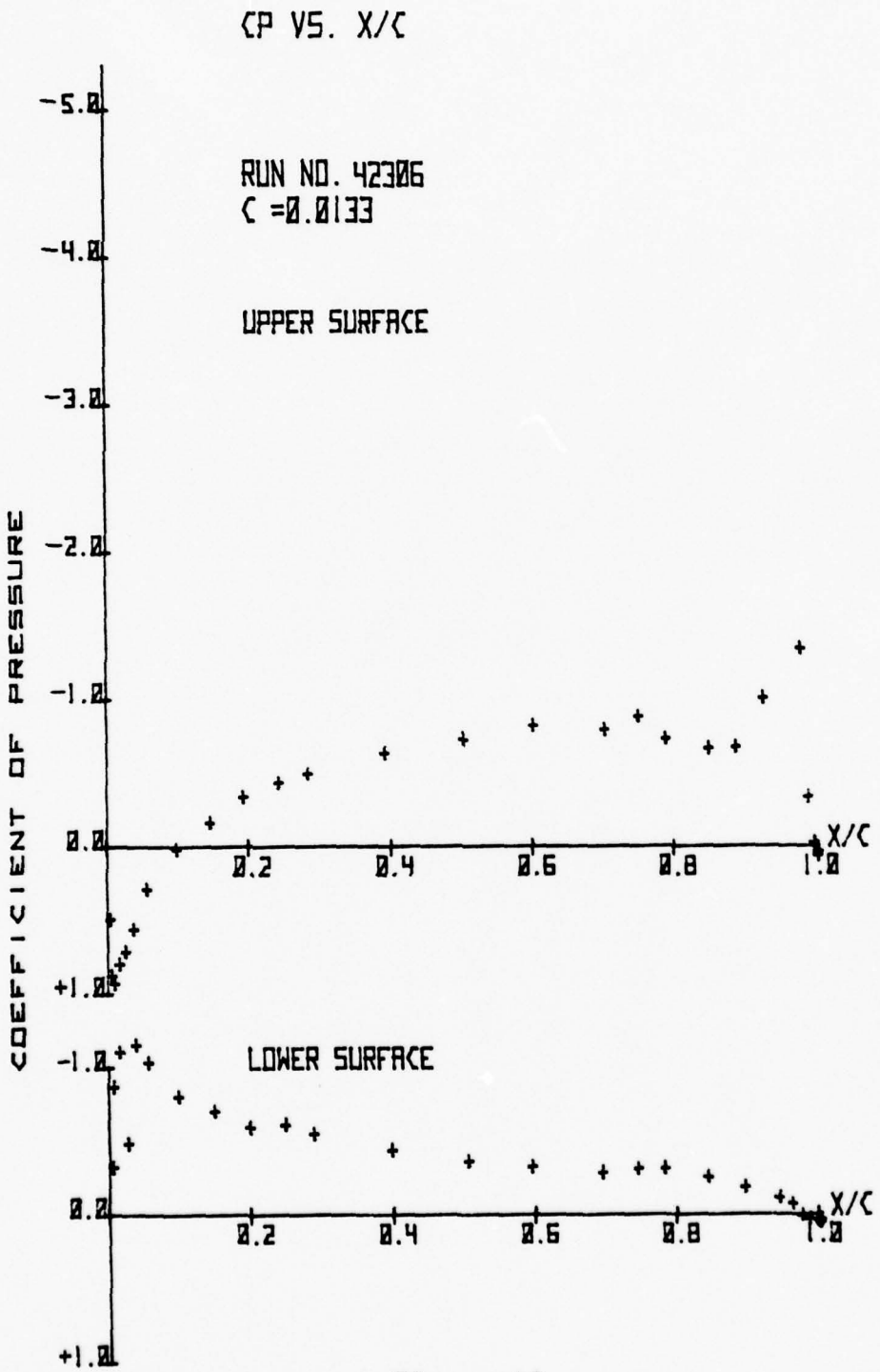
CP VS. X/C
RUN NO. 42306
C =0.0133
UPPER SURFACE
LOWER SURFACE
COEFFICIENT OF PRESSURE
-5.0
-4.0
-3.0
-2.0
-1.0
0.0
+1.0
-1.0
0.2
+1.0
0.2
0.4
0.6
0.8
1.0
X/C
X/C

Figure 12

Also, the low drag qualities of the airfoil are favorable when full thrust recovery of the momentum blowing coefficient is assumed. Pressure coefficient data are listed in Appendix B.

B. UNSTEADY DATA RESULTS

The unsteady aerodynamics of the elliptically shaped airfoil have been given a rather cavalier treatment in the past but their contribution to the total forces and moments must be realized. The implications of the unsteady aerodynamics is not generally well understood; therefore, a simple example is presented here to emphasize their importance before discussion of the unsteady results.

Consider an airfoil at zero angle of attack with the RMS pressure distribution equal on the upper and lower surfaces (Figure 13a) but with unequal relative phase angles (Figure 13b) taken from the quarter-chord and the three-quarter-chord positions from the actual unsteady data (Figure 5). The unsteady normal force coefficient, $\langle C_n^2 \rangle^{\frac{1}{2}}$, is calculated from the numerical approximation to Eq. 3.3, as:

$$\langle C_n^2 \rangle^{\frac{1}{2}} \sin\phi = 0.5(\sin(210^o)+\sin(230^o)-\sin(35^o)-\sin(55^o))$$

$$\langle C_n^2 \rangle^{\frac{1}{2}} \sin\phi = -1.33$$

$$\langle C_n^2 \rangle^{\frac{1}{2}} \cos\phi = 0.5(\cos(210^o)+\cos(230^o)-\cos(35^o)-\cos(55^o))$$

$$\langle C_n^2 \rangle^{\frac{1}{2}} \cos\phi = -1.45$$

$$\langle C_n^2 \rangle^{\frac{1}{2}} = \sqrt{1.33^2 + 1.45^2} \qquad \phi = \frac{-1.33}{-1.45}$$

$$\langle C_n^2 \rangle^{\frac{1}{2}} = 1.97 \qquad \phi = 223^o$$

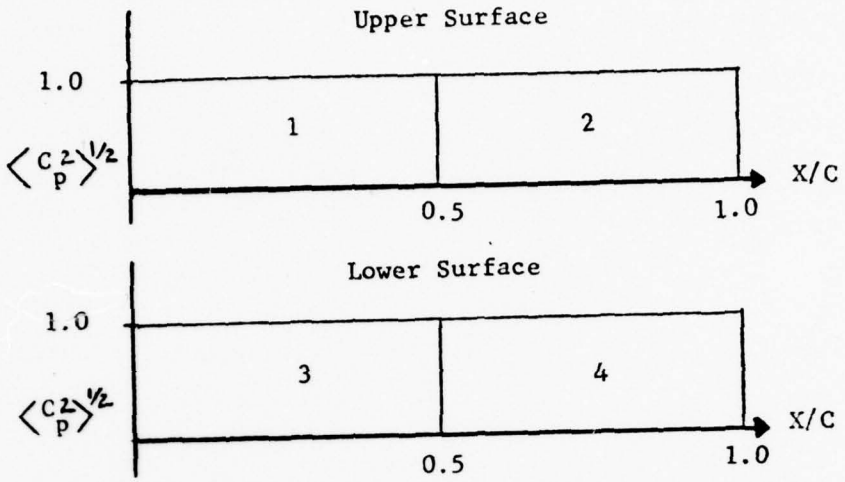

Figure 13a

Region	Phi
1	35 degrees
2	55 degrees
3	210 degrees
4	230 degrees

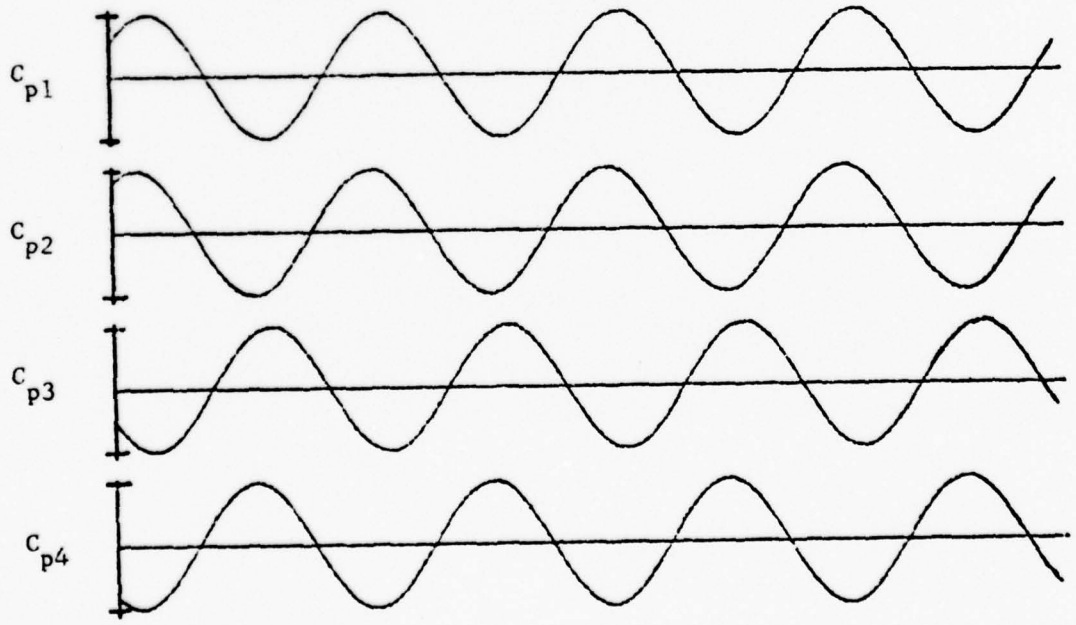

Figure 13b
Sample Pressure Distribution

Similarly, for the moment coefficient (referenced to the trailing edge):

$$\langle C_m^2 \rangle^{\frac{1}{2}} \sin\phi = 0.5((\sin(210^o)-\sin(35^o))0.75+(\sin(230^o)-\sin(55^o))0.25)$$

$$\langle C_m^2 \rangle^{\frac{1}{2}} \sin\phi = -0.6$$

$$\langle C_m^2 \rangle^{\frac{1}{2}} \cos = 0.5((\cos(210^o)-\cos(35^o))0.75+(\cos(230^o)-\cos(55^o))0.25)$$

$$\langle C_m^2 \rangle^{\frac{1}{2}} \cos = -0.78$$

$$\langle C_m^2 \rangle^{\frac{1}{2}} = \sqrt{0.6^2 + 0.78^2} \qquad \phi = \frac{-0.6}{-0.78}$$

$$\langle C_m^2 \rangle^{\frac{1}{2}} = 0.98 \qquad \phi = 217^o$$

Clearly, the force and moment coefficients are of significant magnitude even if a uniform distribution (RMS) of pressure coefficient were assumed, because of the importance of considering relative phase relationships. The dynamic behavior of the unsteady aerodynamics of the circulation control airfoil, particularly the lift amplification ratio, in the unsteady environment caused by cyclic blowing will be investigated after the improved data acquisition system is operational.

As discussed in Section I, measurements were taken in November 1976, with the airfoil experiencing harmonic pressure variations. The unsteady data are listed in Appendix C. The experimental data were numerically integrated, similar to the previous example, for the lift, drag, and pitching moment coefficients (Figures 14 and 15). It should be recognized that the phase shift between the upper

and lower surfaces is approximately 180 degrees, the result being the relatively large amplitude of the aerodynamic coefficients. Highlights of the unsteady results, summarized in Table II, were that:

1. The time varying pressures over the model were predominantly harmonic, with a non-dimensional frequency (Strouhal no.) of

$$S = \frac{f\ t}{U} = 0.449.$$

2. The RMS value of the normal force coefficient was approximately 2.14, which was an order of magnitude greater than the RMS drag coefficient.

3. The test Reynolds no. was approximately

$$R_e = 0.54 \times 10^6.$$

4. The location on the airfoil for the center of pressure due to unsteady loadings was approximately 0.491 chord and the RMS value of pitching moment at this reference point was

$$\langle C_m{}^2 \rangle^{\frac{1}{2}} = 0.1694$$

with a phase angle of 90 degrees lag relative to the normal force. This term may be considered as an apparent mass type effect.

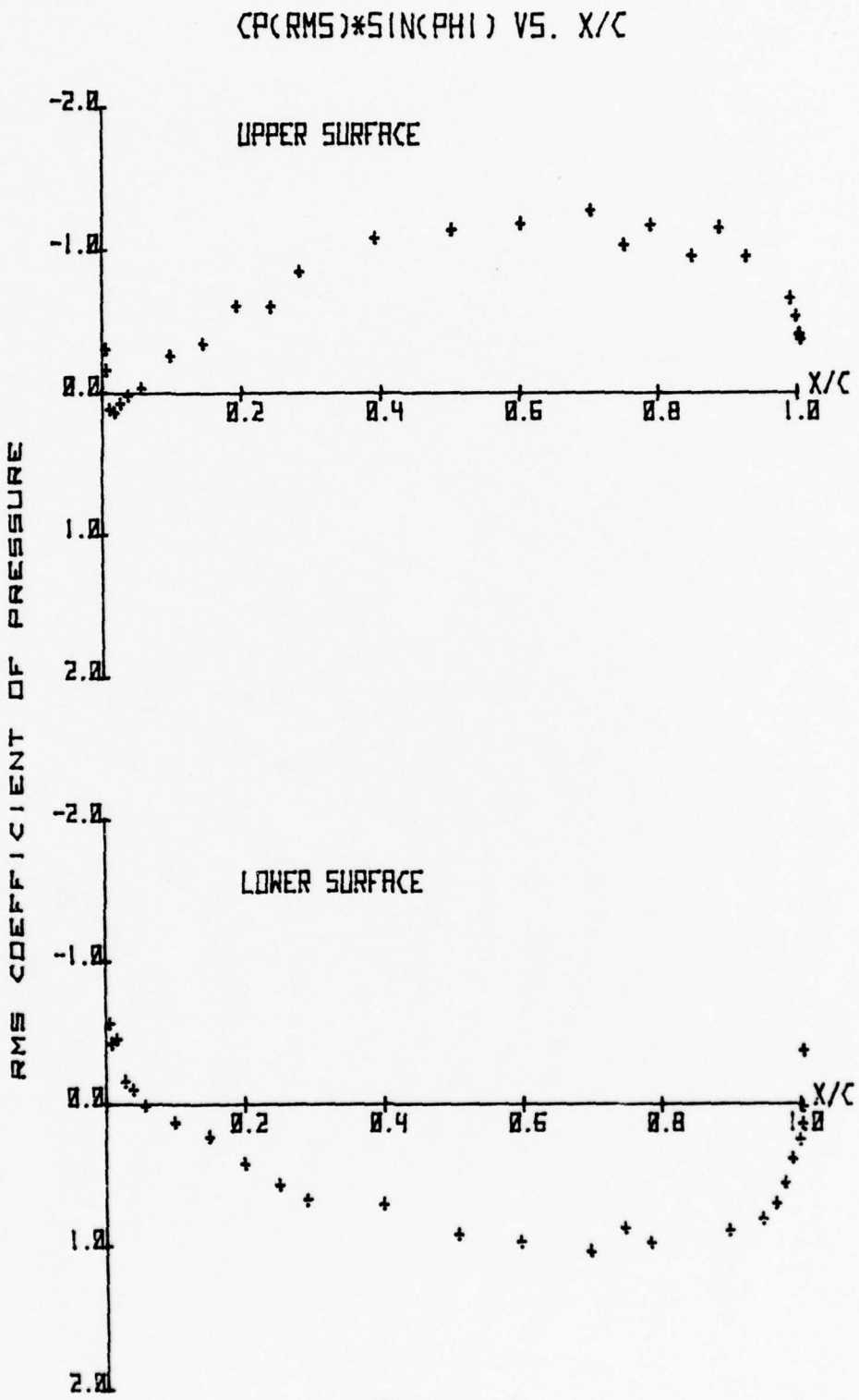
CP(RMS)*SIN(PHI) VS. X/C
UPPER SURFACE
LOWER SURFACE
RMS COEFFICIENT OF PRESSURE
X/C
X/C
-2.0
-1.0
0.0
1.0
2.0
0.2
0.4
0.6
0.8
1.0

Figure 14

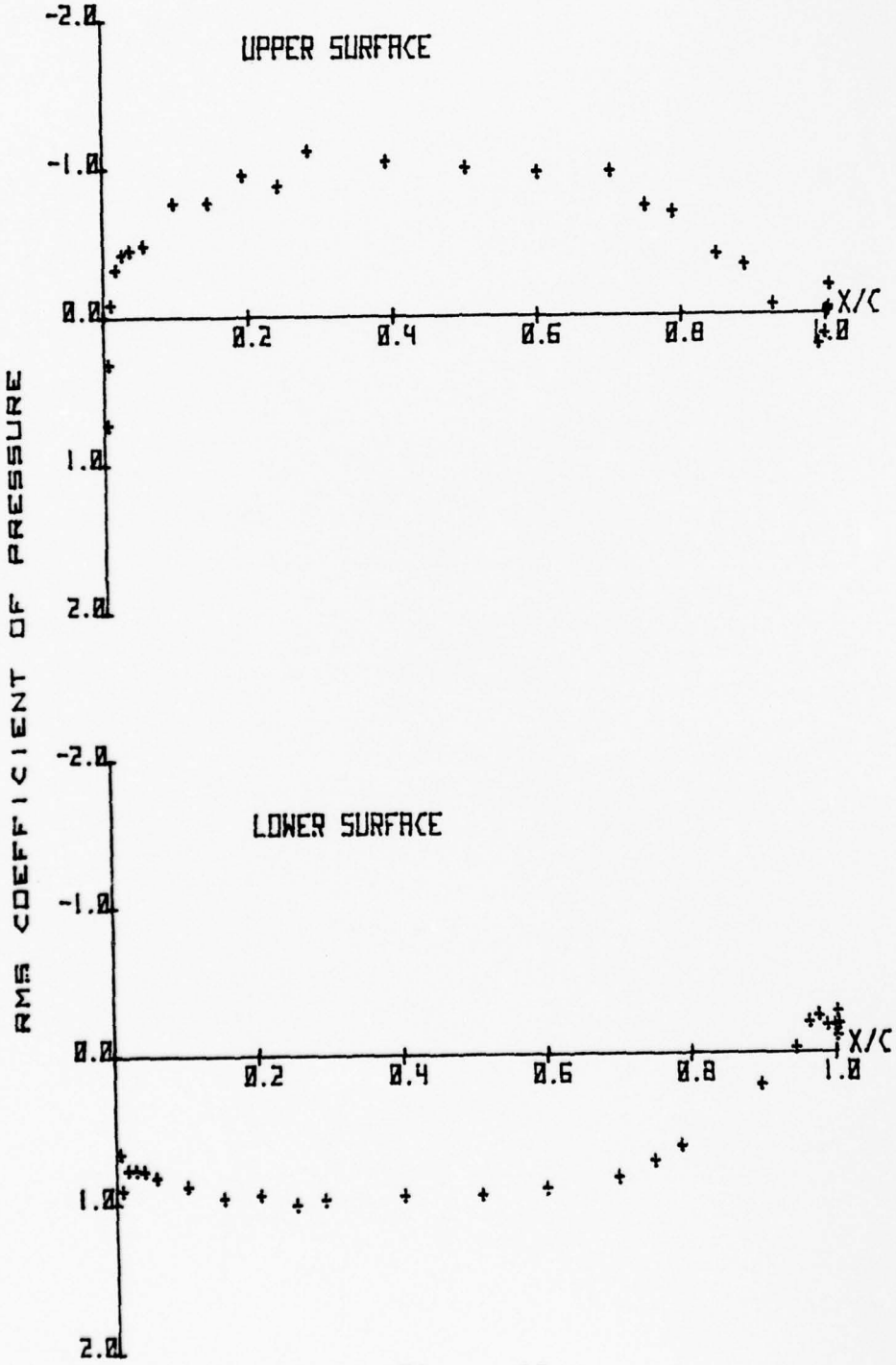
CP(RMS)*COS(PHI) VS. X/C
UPPER SURFACE
LOWER SURFACE
RMS COEFFICIENT OF PRESSURE
-2.0
-1.0
0.0
1.0
2.0
0.2
0.4
0.6
0.8
1.0
X/C

Figure 15

V. DATA REDUCTION FOR THE ADVANCED DATA REDUCTION SYSTEM

The advanced data acquisition system described in Section II C will allow a more comprehensive investigation of the unsteady aerodynamics of the model, but the data reduction techniques must be tailored to handle the large numbers of data to be collected. Oscillation of the plenum pressure as described by Bauman (Reference 6) induces harmonic blowing from the trailing edge slot at a specified frequency, W_1. It is assumed that the unsteady static pressure at each station will have a steady value plus a periodic value with frequency W_1 superimposed due to the oscillating momentum blowing coefficient.

Since the data are assumed periodic in form, the unsteady pressure at any point on the airfoil may be defined by a Fourier series (Ref. 7) as follows:

$$P(x,t)=A_o(x)+\sum_{n=1}^{\infty}\left[A_n(x)\cos(nW_1t)+B_n(x)\sin(nW_1t)\right] \qquad (5.1)$$

where W_1 is the frequency of the oscillation. The standard formulae for obtaining the Fourier coefficients for the infinite series are:

$$A_o(x) = \frac{1}{2T}\int_{-T}^{T} P(x)dx$$

$$A_n(x) = \frac{1}{T}\int_{-T}^{T} P(x)\cos(nx)dx \qquad (5.2)$$

$$B_n(x) = \frac{1}{T}\int_{-T}^{T} P(x)\sin(nx)dx$$

Because the experimental data are in the form of a discritization of a truncated periodic signal, the above equations are slightly altered for estimating the Fourier coefficients. The modified form is:

$$\tilde{A}_o(x) = \frac{1}{K} \sum_{i=1}^{K} P_i(x)$$

$$\tilde{A}_n(x) = \frac{2}{K} \sum_{i=1}^{K} P_i(x)\cos(nW_1 t) \quad ; \quad n=1,\ldots,n \qquad (5.3)$$

$$\tilde{B}_n(x) = \frac{2}{K} \sum_{i=1}^{K} P_i(x)\sin(nW_1 t)$$

where k is the number of samples to be analyzed and n is the harmonic number. It is recognized that the physical meaning of $A_o(x)$ is the steady or mean value of the oscillating pressure. That is, $A_o(x) = \langle p_o(x) \rangle$ where

$$\langle P_o(x) \rangle \equiv \lim_{T \to \infty} \frac{1}{2T} \int_{-T}^{T} P(x)dx \qquad (5.4)$$

By subtracting out the mean pressure value, the signal becomes biased to a pure oscillating pressure with a mean value equal to zero. The terms $\tilde{A}_n(x)$ and $\tilde{B}_n(x)$ are equivalent to the cosine and sine components, respectively, discussed in Section III B. Figure 16 illustrates the reconstruction of a discritized signal utilizing this algorithm programmed on the Hewlett-Packard 9830 calculator (program listing in Appendix A). The error was minimized by insuring that the number of samples analyzed was an integer multiple of the frequency; however, the truncation error was never greater than 2%.

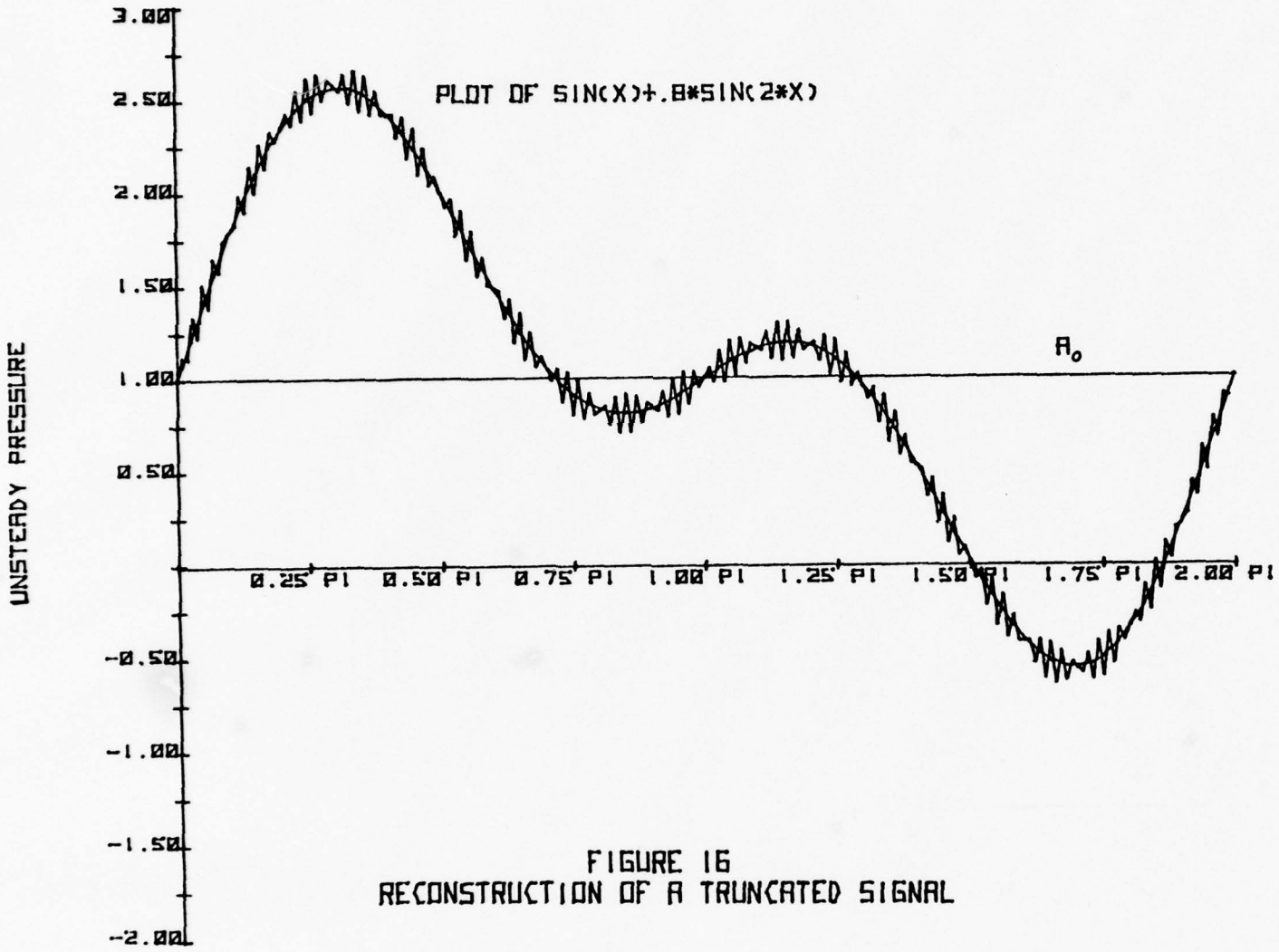

FIGURE 16
RECONSTRUCTION OF A TRUNCATED SIGNAL

Having developed an effective method for handling the large numbers of data, calculation of the aerodynamic force and moment coefficients can be accomplished. Before the actual processing of data begins, the sample pressures are converted to non-dimensional coefficient form to expedite calculations. The unsteady pressure coefficients are

$$C_{p_i}(t) = \frac{Pi-P}{P-H} \qquad i = 1,2,3,\ldots,53 \qquad (5.5)$$

where P and H are steady pressure values from a pitotstatic tube mounted on the floor of the wind tunnel. Then the oscillating signal at any pressure tap is;

$$C_p(x,t) = \Sigma\ A_n \cos(nw_1 t) + B_n \sin(nw_1 t)$$

$$C_p(x,t) = \Sigma\ T_n \sin(nw_1 t + \phi_n) \qquad (5.6)$$

where $T_n = \sqrt{A_n^2 + B_n^2}$, $\phi_n = {}^{B_n}/_{A_n}$.

The unsteady $C_p(x,t)$ are related by the phase angles ϕ , however, the phase angles are meaningless unless they are measured relative to a "clock" or reference signal. Therefore, it is necessary to designate one pressure tap to be used as the reference. Then, the relative phase angle is

$$\phi_{rel} = \phi_i - \phi_{ref} \qquad (5.7)$$

For simplicity, ϕ_i shall hereafter be interpreted as the relative phase angle.

With the steady pressure coefficient removed from the oscillating signal, separate aerodynamic coefficients can be calculated for the steady and unsteady signals. The

steady force and moment coefficients are found exactly as in Section III A. The unsteady aerodynamic coefficients can be defined in a Fourier series form as:

$$C_n(t) = \Sigma\, C_{n_k} \sin(kw_1 t+\phi_k)$$
$$C_c(t) = \Sigma\, C_{c_k} \sin(kw_1 t+\phi_k) \qquad (5.8)$$
$$C_m(t) = \Sigma\, C_{m_k} \sin(kw_1 t+\phi_k)$$

The magnitudes and phase angles of the coefficients can be determined thusly:

for the first harmonic

$$C_{n_1}\sin(w_1 t+\phi) = C_{n_1}\sin\phi\cos(w_1 t)+C_{n_1}\cos\phi\sin(w_1 t)$$

where

$$C_{n_1}\sin\phi = \int_0^1 \left[C_{p_l}(\tfrac{x}{c})\sin\phi_l(\tfrac{x}{c}) - C_{p_u}(\tfrac{x}{c})\sin\phi_u(\tfrac{x}{c})\right] d(\tfrac{x}{c})$$

$$C_{n_1}\cos\phi = \int_0^1 \left[C_{p_l}(\tfrac{x}{c})\cos\phi_l(\tfrac{x}{c}) - C_{p_u}(\tfrac{x}{c})\cos\phi_u(\tfrac{x}{c})\right] d(\tfrac{x}{c}) \qquad (5.9)$$

then

$$C_{n_1} = \sqrt{(C_{n_1}\cos\phi_1)^2 + (C_{n_1}\sin\phi_1)^2}, \qquad \phi_1 = \mathrm{Tan}^{-1}\left(\frac{C_{n_1}\sin\phi_1}{C_{n_1}\cos\phi_1}\right)$$

Similar calculations are done to obtain values for the higher harmonics ($C_{n_2}, C_{n_3}, \cdots, C_{n_i}$) as well as the chord force and pitching moment coefficients using the higher harmonics of pressure coefficient information as obtained during the initial data reduction previously described.

VI. CONCLUSIONS

As mentioned in Section I, the two-fold objective of this paper was to develop a computer program for unsteady aerodynamic analysis and to demonstrate its capabilities on experimentally generated unsteady data. The objective was partially satisfied; a computer program, well within the limitations of mini-calculators such as the Hewlett-Packard 9830, was developed which employed a straightforward numerical integration of pressure coefficients to obtain values for the aerodynamic coefficients. The program can be modified for unsteady data by properly taking into account the cosine and sine components of the pressure signal relative to a fixed harmonic (clock) signal. Also, the extraction of the Fourier coefficients of the truncated, time-varying signal appears to be within the capabilities of the updated data acquisition system.

APPENDIX A

COMPUTER PROGRAM LISTINGS AND OUTPUT

```
  1 REM PROGRAM FOR DECOMPOSITION OF A FUNCTION
  2 REM INTO FOURIER COEFFICIENTS
 10 DIM E[256]
 30 W1=(20*PI)
 35 DISP "DIVISIONS PER CYCLE?";
 36 INPUT D
 42 P=2*PI/W1
 43 T=P/D
 50 REM COMPUTE SAMPLE FUNCTION
 60 FOR I=1 TO 220
 65 X=W1*(I-1)*T
 70 E[I]=SIN(X)+0.5*SIN(2*X)+0.3*SIN(3*X)
 80 NEXT I
100 PRINT
105 PRINT "THE DRIVING FREQUENCY IS 10 HZ"
106 PRINT D; "DIVISIONS PER CYCLE"
107 PRINT
110 PRINT "    COEFFICIENTS"
111 PRINT
113 PRINT TAB2"COS"TAB15"SIN"
114 FOR J=1 TO 3
115 PRINT
117 PRINT TAB2"A";J, "B";J, "PHASE ANGLE"
119 A1=B1=0
120 FOR I=1 TO 220
130 B1=(B1+E[I]*SIN(J*W1*(I-1)*T))
140 A1=(A1+E[I]*COS(J*W1*(I-1)*T))
150 NEXT I
159 P=ATN(B1/A1)
160 WRITE (15,170)(A1*2/220), (B1*2/220), (P*180/PI)
170 FORMAT F6.3,7X,F6.3,13X,F5.1
175 NEXT J
180 END
```

```
THE DRIVING FREQUENCY IS 10 HZ
     10 DIVISIONS PER CYCLE

  COEFFICIENTS
 COS          SIN

 A 1          B 1          PHASE ANGLE
0.000        1.000             90.0

 A 2          B 2          PHASE ANGLE
0.000        0.500             90.0

 A 3          B 3          PHASE ANGLE
0.000        0.300             90.0
```

```
  1 REM COMPUTE CL,CD,CM--STEADY AND UNSTEADY
  2 REM FROM CP DATA ON TAPE CASSETTE
 10 COM R1,D[80],P[80],C[60]
 20 DIM A[106]
 30 PRINT
 40 LOAD DATA 4,A
 60 C9=0
 70 X9=0.95
 80 Y9=0.048
 90 DISP "CP DATA FILE NO. IS";
100 INPUT Z
110 LOAD DATA Z
111 D[22]= 0.4
112 D[36]=0.539
113 G1=1
115 PRINT "INPUT OPTION"
116 PRINT "1 FOR STEADY DATA"
117 PRINT "2 FOR NON-STEADY DATA"
118 INPUT G3
119 GOTO G3 OF 130,212
120 GOTO 130
130 PRINT
140 PRINT "RUN NO. IS"R1
150 PRINT TAB7"UPPER"TAB24"LOWER"
160 PRINT TAB2"N"TAB9"CP"TAB19"N"TAB26"CP"
170 FORMAT F3.0,2X,F7.3,5X,F3.0,2X,F7.3
180 FOR N=1 TO 27
190 M=N+26
200 WRITE (15,170)N,C[N],M,C[M]
201 NEXT N
202 FIXED 3
203 PRINT "CP1="C9"AT X/C="X9", Y/C="Y9
204 STANDARD
205 DISP "CORRECT THE CP VALUES"
206 STOP
210 GOTO 270
212 DISP "INPUT DYNAMIC GAIN";
213 INPUT G2
214 FIXED 3
216 PRINT "RUN NO. IS"R1
217 C9=C[21]+0.33*(C[22]-C[21])
218 PRINT "TAP"TAB7"CP(MEAN)"TAB17"CP(RMS)"TAB27"PHI"
220 FORMAT F3.0,3X,F7.3,3X,F7.3,3X,F4.0
222 FOR I=1 TO 53
224 WRITE (15,220)I,C[I],D[I],P[I]
226 NEXT I
227 PRINT "C9="C9
228 DISP "CORRECT THE CP VALUES"
230 STOP
235 GOTO 270
240 FOR I=1 TO 53
242 C[I]=G2*D[I]*SIN(P[I]/57.296)
244 NEXT I
245 C9=(D[21]+0.33*(D[22]-D[21]))
246 G1=2
247 GOTO 270
```

```
250 FOR I=1 TO 53
252 C[I]=G2*D[I]*COS(P[I]/57.296)
254 NEXT I
256 C9=(D[21]+0.33*(D[22]-D[21]))
257 G1=3
258 GOTO 270
270 L1=0
272 L2=0
274 P1=0
276 P2=0
310 FOR I=1 TO 26
320 IF I=21 THEN 490
330 C1=-C[I]
340 C2=-C[I+1]
350 X1=A[I]
360 X2=A[I+1]
370 GOSUB 1120
380 L1=L1+N1
390 P1=P1+M1
400 C1=C[I+27]
410 C2=C[I+26]
420 X1=A[I+27]
430 X2=A[I+26]
440 GOSUB 1120
450 L2=L2+N1
460 P2=P2+M1
470 NEXT I
480 GOTO 640
490 C1=-C[21]
500 C2=-C9
510 X1=A[21]
520 X2=X9
530 GOSUB 1120
540 L1=L1+N1
550 P1=P1+M1
560 C1=-C9
570 C2=-C[22]
580 X1=X9
590 X2=A 22
600 GOSUB 1120
610 L1=L1+N1
620 P1=P1+M1
630 GOTO 400
640 D1=0
650 D2=0
660 P3=0
670 P4=0
680 FOR I=1 TO 13
690 C1+C[I]
700 C2=C[I+1]
710 Y1=A[I+53]
720 Y2=A[I+54]
730 GOSUB 1160
740 D1=D1+N1
750 P3=P3+M1
760 NEXT I
```

```
 770 FOR I=40 TO 52
 780 C1=C[I]
 790 C2=C[I+1]
 800 Y1=A[I+53]
 810 Y2=A[I+54]
 820 GOSUB 1160
 830 D1=D1+N1
 840 P3=P3+M1
 850 NEXT I
 860 FOR I=14 TO 39
 870 IF I=21 THEN 970
 880 C1=-C[I+1]
 890 C2=C[I]
 900 Y1=A[I+54]
 910 Y2=A[I+53]
 920 GOSUB 1160
 930 D2=D2+N1
 940 P4=P4+M1
 950 NEXT I
 960 GOTO 1200
 970 C1=-C9
 980 C2=C 21
 990 Y1=Y9
1000 Y2=A 74
1010 GOSUB 1160
1020 D2=D2+N1
1030 P4=P4+M1
1040 C1=-C[22]
1050 C2=-C9
1060 Y1=A[75]
1070 Y2=Y9
1080 GOSUB 1160
1090 D2=D2+N1
1100 P4=P4+M1
1110 GOTO 950
1120 M1=C1*(X2-X1)*(1-0.5*(X2+X1)
1130 M1=M1+(C2-C1)*(X2-X1)*(0.5-(X2/3)-(X1/6))
1140 N1=0.5*(C2+C1)*(X2-X1)
1150 RETURN
1160 N1=0.5*(C2+C1)*(Y2-Y1)
1170 M1=0.5*C1*(Y2-Y1)*(Y2+Y1)
1180 M1=M1+(C2-C1)*(Y2-Y1)*((Y1/6)+(Y2/3))
1190 RETURN
1200 PRINT
1205 GOTO G1 OF 1210,1500,1600
1210 PRINT "RUN NO. IS"R1
1220 PRINT
1225 FIXED 4
1230 PRINT "COEFFICIENT BUILDUP IS"
1250 PRINT TAB2"CNU="L1
1260 PRINT TAB2"CNL="L2
1270 PRINT TAB10"TOTAL CN="(L1+L2)
1280 PRINT TAB2"CCF="D1
1290 PRINT TAB2"CCR="D2
1300 PRINT TAB10"TOTAL CC="(D1+D2)
```

```
1310 PRINT TAB2"CMU="P1
1320 PRINT TAB2"CML="P2
1330 PRINT TAB2"CMF="P3
1340 PRINT TAB2"CMR="P4
1350 PRINT TAB10"TOTAL CM="(P1+P2+P3+P4)"AT T.E."
1360 M1=(P1+P2+P3+P4)
1370 N1=(L1+L2)
1380 C1=(D1+D2)
1390 M5=M1-(0.75*N1)
1400 DISP "INPUT ANGLE OF ATTACK (DEGS.)";
1410 INPUT A2
1415 A2=0.01745*A2
1416 A9=A2
1420 N5=N1*COS(A2)-C1*SIN(A2)
1430 C5=C1*COS(A2)+N1*SIN(A2)
1440 PRINT
1445 C2=A2*57.296
1450 PRINT TAB 2"CL(MEAN)="N5;TAB21"CD(MEAN)="C5;
1460 PRINT TAB2"ALPHA ="C2"DEGS"
1470 STANDARD
1480 GOTO G3 OF 90,240,250
1490 END
1500 N3=L1+L2
1502 C3=D1+D2
1504 M3+P1+P2+P3+P4
1505 FIXED 4
1506 PRINT "CN(RMS)*SIN(PHI)="N3
1508 PRINT "CC(RMS)*SIN(PHI)="C3
1510 PRINT "CM(RMS)*SIN(PHI)="M3
1511 PRINT
1595 GOTO 250
1600 N4=L1+L2
1602 C4=D1+D2
1604 M4=P1+P2+P3+P4
1605 FIXED 4
1606 PRINT "CN(RMS)*COS(PHI)="N4
1608 PRINT "CC(RMS)*COS(PHI)="C4
1610 PRINT "CM(RMS)*COS(PHI)="M4
1611 PRINT
1612 N1=SQR(N3↑2+N4↑2)
1613 P1=ATN(N3/N4)
1614 X=N3
1615 Y=N4
1616 F=P1
1617 GOSUB 1900
1618 P1=F
1620 PRINT "CN(RMS)="N1,"PHI="P1*57.296
1630 C1=SQR(C3↑2+C4↑2)
1640 P2=ATN(C3/C4)
1641 X=C3
1642 Y=C4
1643 F=P2
1644 GOSUB 1900
1645 P2=F
1650 PRINT "CC(RMS)="C1,"PHI="P2*57.296
1660 M1=SQR(M3↑2+M4↑2)
```

```
1670 P3=ATN(M3/M4)
1671 X=M3
1672 Y=M4
1673 F=P3
1674 GOSUB 1900
1675 P3=F
1680 PRINT "CM(RMS)="M1,"PHI="P3*57.296
1690 A1=N1*COS(A9)*SIN(P1)-C1*SIN(A9)*SIN(P2)
1700 B1=N1*COS(A9)*COS(P1)-C1*SIN(A9)*COS(P2)
1710 L9=SQR(A1↑2+B1↑2)
1720 L8=ATN(A1/B1)
1721 X=A1
1722 Y=B1
1723 F=L8
1724 GOSUB 1900
1725 L8=F
1730 A2=N1*SIN(A9)*SIN(P1)+C1*COS(A9)+SIN(P2)
1740 B2=N1*COS(P1)*SIN(A9)+C1*COS(A9)*COS(P2)
1750 D9=SQR(A2↑2+B2↑2)
1760 D8=ATN(A2/B2)
1761 X=A2
1762 Y=B2
1763 F=D8
1764 GOSUB 1900
1765 D8=F
1770 A3=M1*SIN(P3)-0.75*N1*SIN(P1)
1780 B3=M1*COS(P3)-0.75*N1*COS(P1)
1790 M9=SQR(A3↑2+B3↑2)
1800 M8=ATN(A3/B3)
1801 X=A3
1802 Y=B3
1803 F=M8
1804 GOSUB 1900
1805 M8=F
1810 PRINT
1820 PRINT TAB10"AERODYNAMIC COEFFICIENT SUMMARY"
1830 PRINT
1840 PRINT "CL="N5" +"L9"SIN(W1*T+"L8*57.296")"
1850 PRINT
1860 PRINT "CD="C5"+"D9"SIN(W1*T+"D8*57.296")"
1870 PRINT
1880 PRINT "CM(C/4)="M5"+"M9"SIN(W1*T+"M8*57.296")"
1890 GOTO 90
1900 IF X<0 AND Y<0 THEN 1920
1910 IF X>0 AND Y<0 THEN 1920
1915 GOTO 1930
1920 F=F+PI
1930 RETURN
1940 STOP
```

STEADY DATA OUTPUT

```
RUN NO. IS 123

COEFFICIENT BUILDUP IS
  CNU= 0.3480
  CNL=-0.4281
          TOTAL CN=-0.0802
  CCF=-0.0339
  CCR= 0.0721
          TOTAL CC= 0.0382
  CMU= 0.1092
  CML=-0.2840
  CMF= 0.0017
  CMR= 0.0038
          TOTAL CM=-0.1693  AT T.E.

  CL(MEAN)=-0.0765  CD(MEAN)= 0.0451    (CM)C/4(MEAN)=-0.1092
  ALPHA =-4.9991  DEGS
```

UNSTEADY DATA OUTPUT

```
CN(RMS)*SIN(PHI)=-1.5385
CC(RMS)*SIN(PHI)=-0.0312
CM(RMS)*SIN(PHI)=-0.6336

CN(RMS)*COS(PHI)=-1.4968
CC(RMS)*COS(PHI)=-0.0042
CM(RMS)*COS(PHI)=-0.8581

CN(RMS)= 2.1465                  PHI=225.7868
CC(RMS)= 0.0315                  PHI=262.2760
CM(RMS)= 1.0667                  PHI=216.4451
```

AERODYNAMIC COEFFICIENT SUMMARY

```
CL=-0.0765  +  2.1405  SIN(W1*T+ 225.8305   )

CD= 0.0451  +  0.1629  SIN(W1*T+  39.2111   )

CM(C/4)=-0.1092  + 0.5836  SIN(W1*T+ 63.0435   )
```

APPENDIX B

PRESSURE COEFFICIENT DATA WITH STEADY ζ_u

RUN NO. 42301 ζ_u=0.00
ANGLE OF ATTACK=-5 DEG U=100 FT/SEC

TAP #	PRESSURE COEFFICIENT	TAP #	PRESSURE COEFFICIENT
1	0.230	28	-0.080
2	0.537	29	-0.115
3	0.928	30	-0.066
4	0.887	31	-0.128
5	0.816	32	-0.107
6	0.706	33	-0.133
7	0.443	34	-0.171
8	0.156	35	-0.186
9	0.006	36	-0.201
10	-0.197	37	-0.261
11	-0.259	38	-0.282
12	-0.353	39	-0.284
13	-0.494	40	-0.339
14	-0.611	41	-0.348
15	-0.655	42	-0.391
16	-0.604	43	-0.503
17	-0.592	44	-0.503
18	-0.591	45	-0.569
19	-0.468	46	-0.672
20	-0.486	47	-0.876
21	-0.390	48	-1.325
22	-0.244	49	-1.399
23	-0.230	50	-0.922
24	-0.075	51	-1.402
25	-0.144	52	-0.940
26	-0.164	53	-0.195
27	-0.118		

PRESSURE COEFFICIENT DATA WITH STEADY C_μ

RUN NO. 42302 C_μ=0.0855
ANGLE OF ATTACK=-5 DEG U=100 FT/SEC

TAP #	PRESSURE COEFFICIENT	TAP #	PRESSURE COEFFICIENT
1	1.000	28	0.116
2	0.974	29	-1.171
3	0.639	30	-1.072
4	0.471	31	-0.504
5	0.233	32	-0.379
6	0.033	33	-0.253
7	-0.186	34	0.013
8	-0.448	35	0.056
9	-0.698	36	0.099
10	-0.818	37	0.061
11	-0.956	38	0.023
12	-1.074	39	-0.105
13	-1.205	40	-0.100
14	-1.274	41	-0.096
15	-1.343	42	-0.172
16	-1.355	43	-0.233
17	-1.372	44	-0.221
18	-1.317	45	-0.259
19	-1.235	46	-0.215
20	-1.190	47	-0.279
21	-3.371	48	-0.363
22	-5.552	49	-0.177
23	-2.814	50	-0.020
24	-0.468	51	0.119
25	-1.154	52	0.453
26	-2.718	53	0.811
27	-2.948		

PRESSURE COEFFICIENT DATA WITH STEADY C_μ

RUN NO. 42303 C_μ=0.0640
ANGLE OF ATTACK=-5 DEG U=100 FT/SEC

TAP #	PRESSURE COEFFICIENT	TAP #	PRESSURE COEFFICIENT
1	1.000	28	0.339
2	0.987	29	0.203
3	0.782	30	-0.895
4	0.541	31	-0.279
5	0.323	32	-0.226
6	0.156	33	-0.151
7	-0.051	34	0.005
8	-0.387	35	0.014
9	-0.484	36	0.023
10	-0.695	37	-0.023
11	-0.815	38	-0.031
12	-0.931	39	-0.097
13	-1.085	40	-0.118
14	-1.160	41	-0.140
15	-1.236	42	-0.228
16	-1.236	43	-0.268
17	-1.165	44	-0.311
18	-1.210	45	-0.296
19	-1.125	46	-0.313
20	-1.051	47	-0.387
21	-2.583	48	-0.584
22	-4.114	49	-0.687
23	-1.880	50	-0.231
24	-0.248	51	0.037
25	-0.718	52	0.117
26	-2.046	53	0.709
27	-1.151		

PRESSURE COEFFICIENT DATA WITH STEADY C_μ

RUN NO. 42304 C_μ=0.0448
ANGLE OF ATTACK=-5 DEG U=100 FT/SEC

TAP #	PRESSURE COEFFICIENT	TAP #	PRESSURE COEFFICIENT
1	0.872	28	0.237
2	1.005	29	0.192
3	0.903	30	-0.238
4	0.665	31	-0.087
5	0.535	32	-0.136
6	0.312	33	-0.164
7	0.090	34	-0.018
8	-0.197	35	-0.036
9	-0.362	36	-0.054
10	-0.519	37	-0.076
11	-0.619	38	-0.105
12	-0.775	39	-0.119
13	-0.928	40	-0.143
14	-1.010	41	-0.167
15	-1.092	42	-0.294
16	-1.026	43	-0.362
17	-1.054	44	-0.367
18	-1.018	45	-0.367
19	-0.867	46	-0.367
20	-0.903	47	-0.534
21	-1.949	48	-0.777
22	-2.994	49	-0.613
23	-1.034	50	-0.297
24	-0.045	51	-0.379
25	-0.229	52	0.090
26	-0.782	53	0.579
27	-0.008		

PRESSURE COEFFICIENT DATA WITH STEADY C_μ

RUN NO. 42305 — C_μ=0.0272
ANGLE OF ATTACK=-5 DEG — U=100 FT/SEC

TAP #	PRESSURE COEFFICIENT	TAP #	PRESSURE COEFFICIENT
1	0.729	28	0.117
2	0.980	29	0.154
3	0.983	30	0.050
4	0.816	31	0.045
5	0.602	32	-0.032
6	0.423	33	-0.082
7	0.268	34	-0.042
8	-0.087	35	-0.065
9	-0.251	36	-0.087
10	-0.418	37	-0.128
11	-0.503	38	-0.186
12	-0.604	39	-0.224
13	-0.756	40	-0.224
14	-0.837	41	-0.224
15	-0.918	42	-0.290
16	-0.893	43	-0.396
17	-0.866	44	-0.432
18	-0.851	45	-0.451
19	-0.691	46	-0.448
20	-0.801	47	-0.609
21	-1.370	48	-0.888
22	-1.940	49	-0.842
23	-0.536	50	-0.749
24	0.057	51	-0.533
25	-0.046	52	-0.262
26	-0.030	53	0.183
27	0.066		

PRESSURE COEFFICIENT DATA WITH STEADY C_μ

RUN NO. 42306 C_μ=0.0133
ANGLE OF ATTACK=-5 DEG U=100 FT/SEC

TAP #	PRESSURE COEFFICIENT	TAP #	PRESSURE COEFFICIENT
1	0.522	28	0.086
2	0.908	29	0.085
3	0.964	30	0.075
4	0.828	31	0.063
5	0.743	32	0.039
6	0.590	33	-0.039
7	0.318	34	-0.080
8	0.046	35	-0.150
9	-0.136	36	-0.220
10	-0.311	37	-0.279
11	-0.407	38	-0.276
12	-0.468	39	-0.251
13	-0.604	40	-0.291
14	-0.697	41	-0.331
15	-0.789	42	-0.407
16	-0.762	43	-0.515
17	-0.850	44	-0.579
18	-0.699	45	-0.563
19	-0.632	46	-0.674
20	-0.641	47	-0.772
21	-0.975	48	-1.003
22	-1.309	49	-1.123
23	-0.306	50	-0.454
24	0.006	51	-1.075
25	0.067	52	-0.838
26	0.097	53	-0.290
27	0.067		

APPENDIX C

UNSTEADY PRESSURE DATA

ANGLE OF ATTACK=-5 DEG U=100 FT/SEC

TAP #	MEAN PRESSURE COEFFICIENT	UNSTEADY PRESSURE COEFFICIENT	PHASE ANGLE
1	0.270	0.404	160
2	0.725	0.186	160
3	0.908	0.079	290
4	0.812	0.168	330
5	0.750	0.203	345
6	0.624	0.210	353
7	0.383	0.225	0
8	0.181	0.384	17
9	-0.048	0.400	23
10	-0.186	0.545	32
11	-0.273	0.513	34
12	-0.352	0.681	37
13	-0.480	0.730	46
14	-0.553	0.737	49
15	-0.626	0.743	51
16	-0.621	0.780	53
17	-0.595	0.613	55
18	-0.597	0.661	60
19	-0.498	0.500	68
20	-0.421	0.582	75
21	-0.367	0.461	88
22	-0.313	0.400	103
23	-0.295	0.338	111
24	-0.283	0.265	109
25	-0.275	0.185	92
26	-0.338	0.188	89
27	-0.425	0.188	65

UNSTEADY PRESSURE DATA

(CONTINUED)

ANGLE OF ATTACK=-5 DEG U=100 FT/SEC

TAP #	MEAN PRESSURE COEFFICIENT	UNSTEADY PRESSURE COEFFICIENT	PHASE ANGLE
28	-0.410	0.125	348
29	-0.285	0.094	295
30	-0.238	0.161	298
31	-0.257	0.223	290
32	-0.181	0.314	290
33	-0.173	0.376	283
34	-0.178	0.421	270
35	-0.192	0.478	255
36	-0.205	0.539	240
37	-0.228	0.600	237
38	-0.243	0.588	230
39	-0.260	0.688	231
40	-0.284	0.684	227
41	-0.308	0.680	224
42	-0.368	0.613	217
43	-0.508	0.613	215
44	-0.558	0.600	210
45	-0.593	0.538	205
46	-0.648	0.513	195
47	-0.853	0.463	190
48	-1.250	0.425	183
49	-1.308	0.405	175
50	-0.983	0.405	171
51	-1.453	0.450	152
52	-1.125	0.508	157
53	-0.335	0.435	142

LIST OF REFERENCES

1. Lockheed - California Company Report LR 26417, Design Study of a Helicopter with a Circulation Control Rotor, by W. D. Anderson, and others, May 1974.

2. Naval Postgraduate School Progress Report No. 3, Circulation Control Airfoil Study, by J. A. Miller and L. V. Schmidt, 25 December 1976.

3. Johnson, R.B., A Technique for Measuring Unsteady Pressures, M.S. Thesis, Naval Postgraduate School, September 1968.

4. Naval Ship Research and Development Center Technical Note AL-211, Two-Dimensional Subsonic Wind Tunnel Tests of Two 15-Percent Thick Circulation Control Airfoils, by Robert J. Englar, August 1971.

5. Naval Ship Research and Development Center Technical Note AL-201, Two-Dimensional Subsonic Wind Tunnel Investigations of a Cambered 30-Percent Thick Circulation Control Airfoil, by Robert J. Englar, May 1972.

6. Bauman, J.L., Development of a Control Valve to Induce an Oscillating Blowing Coefficient in a Circulation Control Rotor, M.S. Thesis, Naval Postgraduate School, December 1976.

7. Kreyszig, E., Advanced Engineering Mathematics, Third Edition, p. 381, John Wiley & Sons, Inc., 1972.

INITIAL DISTRIBUTION LIST

		No. Copies
1.	Defense Documentation Center Cameron Station Alexandria, Virginia 22314	2
2.	Library, Code 0142 Naval Postgraduate School Monterey, California 93940	2
3.	Department Chairman, Code 67 Department of Aeronautics Naval Postgraduate School Monterey, California 93940	1
4.	Professor Louis V. Schmidt, Code 67Sx Department of Aeronautics Naval Postgraduate School Monterey, California 93940	1
5.	Professor James A. Miller, Code 67Mo Department of Aeronautics Naval Postgraduate School Monterey, California 93940	1
6.	Commanding Officer Attn: Mr. R. F. Siewert, AIR-320D Naval Air Systems Command Washington, D.C. 20361	1
7.	Commanding Officer Attn: Dr. H. Chaplin, Code ASED David W. Taylor Naval Ship Research and Development Center Bathesda, Maryland 20034	1
8.	LT Billy M. Pickelsimer, USN 515 Shell Street Healdton, Oklahoma 73438	1